

# The P2 Experiment

## A future high-precision measurement of the electroweak mixing angle at low momentum transfer

Dominik Becker<sup>1,2</sup>, Razvan Bucoveanu<sup>1,3</sup>, Carsten Grzesik<sup>1,2</sup>, Ruth Kempf<sup>1,2</sup>, Kathrin Imai<sup>1,2</sup>, Matthias Molitor<sup>1,2</sup>, Alexey Tyukin<sup>1,2</sup>, Marco Zimmermann<sup>1,2</sup>, David Armstrong<sup>4</sup>, Kurt Aulenbacher<sup>1,2,5</sup>, Sebastian Baunack<sup>1,2</sup>, Rakitha Beminiwattha<sup>6</sup>, Niklaus Berger<sup>1,2</sup>, Peter Bernhard<sup>1,7</sup>, Andrea Brogna<sup>1,7</sup>, Luigi Capozza<sup>1,2,5</sup>, Silviu Covrig Dusa<sup>8</sup>, Wouter Deconinck<sup>4</sup>, Jürgen Diefenbach<sup>1,2</sup>, Jens Erler<sup>9</sup>, Ciprian Gal<sup>10</sup>, Boris Gläser<sup>1,2</sup>, Boxing Gou<sup>1,2,5</sup>, Wolfgang Gradl<sup>1,2</sup>, Michael Gericke<sup>11</sup>, Mikhail Gorchtein<sup>1,2</sup>, Yoshio Imai<sup>1,2</sup>, Krishna S. Kumar<sup>12</sup>, Frank Maas<sup>1,2,5,a</sup>, Juliette Mammei<sup>11</sup>, Jie Pan<sup>11</sup>, Preeti Pandey<sup>11</sup>, Kent Paschke<sup>10</sup>, Ivan Perić<sup>13</sup>, Mark Pitt<sup>14</sup>, Sakib Rahman<sup>11</sup>, Seamus Riordan<sup>15</sup>, David Rodríguez Piñeiro<sup>1,2,5</sup>, Concettina Sfienti<sup>1,2,3,7</sup>, Iurii Sorokin<sup>1,2</sup>, Paul Souder<sup>16</sup>, Hubert Spiesberger<sup>1,3</sup>, Michaela Thiel<sup>1,2</sup>, Valery Tyukin<sup>1,2</sup>, and Quirin Weitzel<sup>1,7</sup>

<sup>1</sup> PRISMA Cluster of Excellence, Johannes Gutenberg-Universität Mainz, Germany

<sup>2</sup> Institute of Nuclear Physics, Johannes Gutenberg-Universität Mainz, Germany

<sup>3</sup> Institute of Physics, Johannes Gutenberg-Universität, Mainz, Germany

<sup>4</sup> College of William and Mary, Williamsburg, Virginia, USA

<sup>5</sup> Helmholtz Institute Mainz, Johannes Gutenberg-Universität Mainz, Germany

<sup>6</sup> Louisiana Tech University, Ruston, Louisiana, USA

<sup>7</sup> Detector Laboratory, PRISMA Cluster of Excellence, Johannes Gutenberg-Universität Mainz, Germany

<sup>8</sup> Thomas Jefferson National Accelerator Facility, Newport News, Virginia, USA

<sup>9</sup> Departamento de Física Teórica, Instituto de Física, Universidad Nacional Autónoma de México, CDMX, México

<sup>10</sup> University of Virginia, Charlottesville, Virginia, USA

<sup>11</sup> Department of Physics and Astronomy, University of Manitoba, Winnipeg, Canada

<sup>12</sup> Department of Physics and Astronomy, Stony Brook University, Stony Brook, USA

<sup>13</sup> Institute for Data Processing and Electronics, Karlsruhe Institute of Technology, Karlsruhe, Germany

<sup>14</sup> Virginia Tech University, Blacksburg, Virginia, USA

<sup>15</sup> Physics Division, Argonne National Laboratory, Argonne, USA

<sup>16</sup> Physics Department, Syracuse University, Syracuse, USA

Received: date / Revised version: date

**Abstract.** This article describes the research and development work for the future P2 experimental facility at the upcoming MESA accelerator in Mainz. The facility is optimized for the detection of order  $10^{-8}$  parity-violating cross section asymmetries in electron scattering. The physics program of the facility comprises indirect, high precision search for physics beyond the Standard Model, measurement of the neutron distribution in nuclear physics, single-spin asymmetries stemming from two-photon exchange and a possible future extension to the measurement of hadronic parity violation.

The first measurement of the P2 experiment for which the research and development work is most advanced is described here in detail. It aims for a high precision determination of the weak mixing angle  $\sin^2 \theta_W$  to a precision of 0.14 % at a four-momentum transfer of  $Q^2 = 4.5 \times 10^{-3} \text{ GeV}^2$ . The accuracy is comparable to existing measurements at the Z pole. It comprises a sensitive test of the standard model up to a mass scale of 50 TeV, extendable to 70 TeV. This requires a measurement of the parity violating cross section asymmetry  $\langle A^{\text{exp}} \rangle = -39.94 \times 10^{-9}$  in the elastic electron-proton scattering with a total accuracy of  $\Delta \langle A^{\text{exp}} \rangle_{\text{Total}} = 0.56 \times 10^{-9}$  (1.4%) in 10 000 h of 150  $\mu\text{A}$  polarized electron beam impinging on a 60 cm  $\ell\text{H}_2$  target allowing for an extraction of the weak charge of the proton which is directly connected to the weak mixing angle  $\sin^2 \theta_W$ . Contributions from  $\gamma\text{Z}$ -box graphs become small at the small beam energy of  $E_{\text{beam}} = 155 \text{ MeV}$ .

The size of the asymmetry is the smallest asymmetry ever measured in electron scattering with an unprecedented goal for the accuracy. The use of a solenoid-spectrometer with 100 %  $\phi$ -acceptance as well as an atomic H trap polarimeter are some new features, which have never before been used in parity-violation experiments, and which we describe among others, here. In order to collect the enormous statistics required for this measurement, the new Mainz Energy Recovery Superconducting Accelerator (MESA) is under construction. The plans on the associated beam control system and the polarimetry is described in this article as well. A new  $\ell\text{H}_2$  high-power target design with an enormously low noise level of 10 ppm needs to be constructed. We report here in addition on the conceptual design of the P2 spectrometer, its Cherenkov detectors, the integrating read-out electronics as well as the ultra-thin, fast tracking detectors. There has been substantial theory work done in preparation of the determination of  $\sin^2 \theta_W$ . The further physics program in particle and nuclear physics is described here as well.

**PACS.** 11.30.Er Charge conjugation, parity, time reversal, and other discrete symmetries – 12.15.Lk Electroweak radiative corrections – 13.85.Dz Elastic scattering – 13.88.+e Polarization in interactions and scattering – 25.30.Bf Elastic electron scattering – 29.20.Ej Linear accelerators – 29.27.Hj Polarized beams – 29.40.Gx Tracking and position-sensitive detectors – 29.40.Ka Cherenkov detectors

# Remote sensing of geomagnetic fields and atomic collisions in the mesosphere

Felipe Pedreros Bustos<sup>\*1</sup>, Domenico Bonaccini Calia<sup>2</sup>, Dmitry Budker<sup>1</sup>, Mauro Centrone<sup>3</sup>, Joschua Hellemeier<sup>4</sup>, Paul Hickson<sup>4</sup>, Ronald Holzlöhner<sup>2</sup>, and Simon Rochester<sup>5</sup>

<sup>1</sup>Johannes Gutenberg University, Helmholtz Institut Mainz, Germany

<sup>2</sup>European Southern Observatory, Germany

<sup>3</sup>INAF – Osservatorio Astronomico di Roma, Italy

<sup>4</sup>University of British Columbia, Canada

<sup>5</sup>Rochester Scientific LLC, El Cerrito, CA

February 14, 2018

## Abstract

Magnetic-field sensing has contributed to the formulation of the plate-tectonics theory, the discovery and mapping of underground structures on Earth, and the study of magnetism in other planets. Filling the gap between space-based and near-Earth observation, we demonstrate a novel method for remote measurement of the geomagnetic field at an altitude of 85–100 km. The method consists of optical pumping of atomic sodium in the upper mesosphere with an intensity-modulated laser beam, and simultaneous ground-based observation of the resultant magneto-optical resonance when driving the atomic-sodium spins at the Larmor precession frequency. The experiment was carried out at the Roque de Los Muchachos Observatory in La Palma (Canary Islands) where we validated this technique and remotely measured the Larmor precession frequency of sodium as 260.4(1) kHz, corresponding to a mesospheric magnetic field of 0.3720(1) G. We demonstrate a magnetometry accuracy level of 0.28 mG/ $\sqrt{\text{Hz}}$  in good atmospheric conditions. In addition, these observations allow us to characterize various atomic-collision processes in the mesosphere. Remote detection of mesospheric magnetic fields has potential applications such as mapping of large-scale magnetic structures in the lithosphere and the study of electric-current fluctuations in the ionosphere.

## 1 Introduction

Laser excitation of the atomic sodium layer, located between 85 and 100 km altitude in the upper mesosphere, allows astronomers to create artificial light sources, known as Laser Guide Stars (LGS), to assist adaptive optics systems [1]. A laser beam tuned to a wavelength resonant with the  $3S_{1/2} \rightarrow 3P_{3/2}$  transition in sodium produces atomic fluorescence that is collected at ground with a telescope for real-time compensation of atmospheric turbulence in astronomical observations. Since the introduction of this technique [2, 3], research has been conducted to optimize laser excitation schemes in order to maximize the flux of photons returned to the ground. This technological progress has also catalyzed new concepts of laser remote sensing of magnetic fields with mesospheric sodium [4]. Because of the proximity of the sodium layer to the D and E regions of the ionosphere (between 70 km to 120 km altitude) mesospheric magnetometry opens the possibility to map local current structures in the dynamo region [5, 6]. In addition, the capability of continuously monitoring the geomagnetic field at altitudes of 85–100 km could provide valuable information for modeling the geomagnetic field, detection of oceanic currents [7], and for mapping and identification of large-scale magnetic structures in the upper mantle [8].

In a laser magnetometer, atoms are optically polarized, and the effects of the interaction of the polarized atoms with magnetic fields are observed [9]. For instance, optical pumping of sodium with left-handed circularly polarized light produces atomic polarization in the  $|F = 2, m = +2\rangle$  ground state (here  $F$  is the total angular momentum in the ground state and  $m$  is the Zeeman sublevel) that is depolarized by the action of magnetic fields due to spin-precession of the atomic angular momentum at the Larmor frequency [10]. If the medium is pumped with light pulses synchronized with the Larmor precession, a high degree of atomic polarization can be obtained and an increase in the fluorescence in the cycling transition  $|F = 2, m = +2\rangle \rightarrow |F' = 3, m' = +3\rangle$  can be observed (the primed quantities refer to the excited atomic state) [11]. The direct measurement of the Larmor frequency ( $f_{\text{Larmor}}$ ) gives the magnetic field  $B$  from  $f_{\text{Larmor}} = \gamma B$ , where  $\gamma$  is the gyromagnetic ratio of ground-state sodium given by  $\gamma = 699\,812\text{ Hz/G}$ . This relationship applies to weak magnetic

<sup>\*</sup>Corresponding author. Email: pedreros@uni-mainz.de

# Preliminary Measurements for a Sub-Femtosecond Electron Bunch Length Diagnostic

M.K. Weikum<sup>a,b,\*</sup>, G. Andonian<sup>c,d</sup>, N.S. Sudar<sup>d</sup>, M.G. Fedurin<sup>e</sup>, M.N. Polyanskiy<sup>e</sup>, C. Swinson<sup>e</sup>, A. Ovodenko<sup>c</sup>, F. O'Shea<sup>c</sup>, M. Harrison<sup>c</sup>, Z.M. Sheng<sup>b</sup>, R.W. Assmann<sup>a</sup>

<sup>a</sup>Deutsches Elektronensynchrotron (DESY), 22607 Hamburg, Germany

<sup>b</sup>SUPA, Department of Physics, University of Strathclyde, G4 0NG Glasgow, United Kingdom

<sup>c</sup>RadiaBeam Technologies, LLC, Santa Monica, CA 90404, USA

<sup>d</sup>Department of Physics and Astronomy, UCLA, Los Angeles, CA 90095, USA

<sup>e</sup>Brookhaven National Laboratory, Long Island, NY 11967, USA

## Abstract

With electron beam durations down to femtoseconds and sub-femtoseconds achievable in current state-of-the-art accelerators, longitudinal bunch length diagnostics with resolution at the attosecond level are required. In this paper, we present such a novel measurement device which combines a high power laser modulator with an RF deflecting cavity in the orthogonal direction. While the laser applies a strong correlated angular modulation to a beam, the RF deflector ensures the full resolution of this streaking effect across the bunch hence recovering the temporal beam profile with sub-femtosecond resolution. Preliminary measurements to test the key components of this concept were carried out at the Accelerator Test Facility (ATF) at Brookhaven National Laboratory recently, the results of which are presented and discussed here. Moreover, a possible application of the technique for novel accelerator schemes is examined based on simulations with the particle-tracking code *elegant* and our beam profile reconstruction tool.

**Keywords:** bunch length diagnostic; sub-femtosecond resolution; RF deflecting cavity; laser modulator; ultrashort beam; longitudinal beam profile

## 1. Introduction

Most common longitudinal electron beam diagnostic techniques today, such as electro-optical measurements, transition radiation measurements and transverse deflecting cavities, are limited in resolution to the single to tens of femtosecond level [1, 2, 3, 4]. This stands in contrast, however, with rapid developments in ultrashort electron beam generation methods aiming at developing bunch lengths in the sub-femtosecond to attosecond range through techniques, like bunch compression [5], microbunching [6] or laser wakefield acceleration [7]. In order to fully characterise such beams longitudinally, current measurement techniques need to be improved or new ones developed, efforts into which in recent years have lead to a range of novel proposals, such as plasma deflectors [8], THz streaking [9] and other phase-space mapping techniques (e.g. [10, 11]), most of which have not been experimentally proven so far.

In this paper we want to report on experimental tests of one such novel diagnostic device, as proposed by Andonian et al. [14]. The machine works by streaking an electron beam both in the horizontal and vertical direction through a combination of a laser modulator – a laser

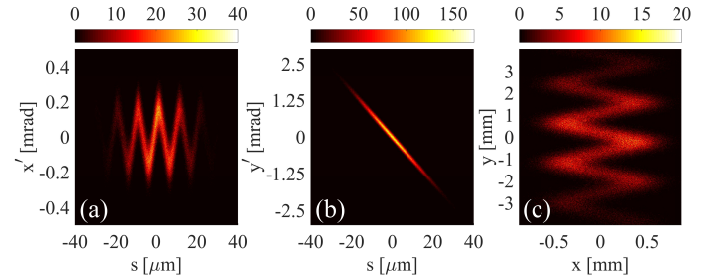


Figure 1: (a-b): Angular kick experienced by the electrons as a function of their longitudinal coordinate  $s$  in the laser modulator (a) and RF deflecting cavity (b). (c): Final transverse beam distribution after the beam has passed through both components and a drift space of 2 m. The color scale shows the electron intensity in arbitrary units. All three plots are generated based on simulations with the tracking code *elegant* [12] and visualisation via *sirepo* [13].

pulse co-propagating with the electrons in an undulator – and an RF transverse deflecting structure (TDS). With the laser pulse in the transverse  $TEM_{10}$ -mode, its interaction with the electron beam in the modulator applies a time-dependent kick to the electrons with amplitude (see Fig. 1(a))

$$\Delta x' = S_{LM} \sin(\omega t + \phi) \quad (1)$$

where  $\omega$  is the laser frequency and  $\phi$  the relative laser-electron phase.  $S_{LM}$  is the streaking amplitude of the

\*Corresponding Author at: DESY, Bdg. 30b, Notkestr. 85, 22607 Hamburg, Germany. Tel.: +49 40 8998 1584.

Email address: maria.weikum@desy.de (M.K. Weikum)

# Interferometer-based high-accuracy white light measurement of neutral rubidium density and gradient at AWAKE

F. Batsch<sup>a,b,c</sup>, M. Martyanov<sup>b</sup>, E. Oez<sup>b</sup>, J. Moody<sup>b</sup>, E. Gschwendtner<sup>a</sup>, A. Caldwell<sup>b</sup>, P. Muggli<sup>a,b</sup>

<sup>a</sup>CERN, Geneva, Switzerland

<sup>b</sup>Max Planck Institute for Physics, Munich, Germany

<sup>c</sup>Technical University Munich, Munich, Germany

## Abstract

The AWAKE experiment requires an automated online rubidium (Rb) plasma density and gradient diagnostic for densities between 1 and  $10 \cdot 10^{14} \text{ cm}^{-3}$ . A linear density gradient along the plasma source at the percent level may be useful to improve the electron acceleration process. Because of full laser ionization of Rb vapor to  $\text{Rb}^+$  within a radius of 1 mm, the plasma density equals the vapor density. We measure the Rb vapor densities at both ends of the source, with high precision using, white light interferometry. At either source end, broadband laser light passes a remotely controlled Mach-Zehnder interferometer built out of single mode fibers. The resulting interference signal, influenced by dispersion in the vicinity of the Rb D1 and D2 transitions, is dispersed in wavelength by a spectrograph. Fully automated Fourier-based signal conditioning and a fit algorithm yield the density with an uncertainty between the measurements at both ends of 0.11 to 0.46 % over the entire density range. These densities used to operate the plasma source are displayed live in the control room.

**Keywords:** Proton driven plasma wakefield, AWAKE, Accurate density and gradient measurement, Rubidium vapor source, Mach-Zehnder interferometer, Fourier-based signal conditioning

## 1. Introduction

The AWAKE project at CERN is a proof-of-concept experiment that uses a proton bunch for particle beam driven plasma wakefield acceleration of electrons [1, 2, 3]. The goal is to reach energies on the scale of several GeV using coherently driven plasma waves with acceleration gradients  $> 1 \text{ GeV/m}$  [4]. The entire process, i.e. modulating the 12 cm long ( $\sigma_z$ ), 400 GeV proton bunch [3] by seeded self-modulation (SSM) [4, 5] into micro bunches, wakefield creation and electron acceleration, happens in a 10 m long, 4 cm diameter rubidium (Rb) vapor source [6, 7, 8], depicted in Fig. 1. At each end, a flask with separately controlled electrical heaters is filled with Rb, providing Rb vapor densities up to  $1 \cdot 10^{15} \text{ cm}^{-3}$ . The baseline density is  $n_{\text{Rb}} = 7 \cdot 10^{14} \text{ cm}^{-3}$  [7]. A fluid heat exchanger with temperature-stabilization surrounds the source and ensures a high temperature and vapor density uniformity ( $< 0.2 \%$ , [6]). An intense laser pulse ionizes the Rb vapor (first  $e^-$  of each Rb atom), forming a 2 mm diameter plasma along the source with equal density and uniformity. By setting different temperatures in the downstream and upstream flasks, a linear vapor / plasma density gradient along the source can be set. Beside the density uniformity, the absolute vapor density and a possible gradient along the source influence the acceleration process [9]. The absolute density determines the proton bunch modulation frequency. Density gradients on the order of  $+1$  to  $+10 \%$  (i.e. the density increases along the 10 m pipe in direction of the beam) can affect the  $e^-$  acceleration in a positive way [9].

We determine the plasma density and gradient by measuring

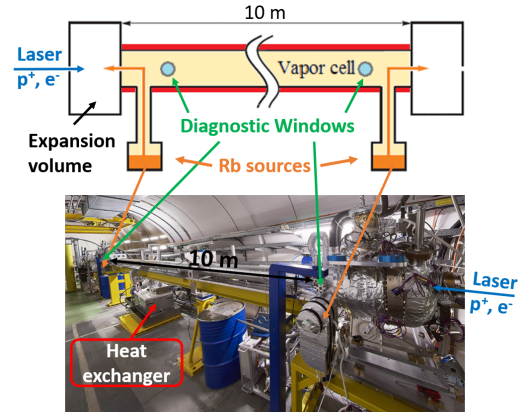


Figure 1: Top: Schematic of the Rb vapor source showing the 10 m long pipe surrounded by the heat exchanger (red), two Rb reservoirs (orange) providing the Rb vapor and 2 diagnostic viewports near the source ends. Bottom: Photo of the AWAKE vapor source. The blue posts at each end are supports for the interferometer optics.

the Rb vapor density through diagnostic windows located at each of the source ends (see Fig. 1) using a Mach-Zehnder interferometer and white light interferometry [10, 11]. To ensure a sufficiently high accuracy in gradient determination, we aim for an uncertainty in measuring the densities at both source ends to better than 1 %. To operate the vapor source remotely, from the control room, while ensuring the required densities and gradients, the diagnostic must allow for a fully automated and remote-controlled operation and provide online density val-

# Required sensitivity to search the neutrinoless double beta decay in $^{124}\text{Sn}$

M. K. Singh,<sup>1,2</sup> V. Sharma,<sup>1,2</sup> A. Kumar,<sup>1</sup> A. Pandey,<sup>1</sup> V. Singh,<sup>1,\*</sup> H.T. Wong,<sup>2</sup>

<sup>1</sup> Department of Physics, Banaras Hindu University, Varanasi 221005, India.

<sup>2</sup> Institute of Physics, Academia Sinica, Taipei 11529, Taiwan.

\*Email: [venkaz@yahoo.com](mailto:venkaz@yahoo.com)

## Abstract

Understanding of particle physics will be incomplete without knowing the true nature i.e. Dirac or Majorana, and absolute effective mass of neutrinos. This will lead us into the world of beyond the standard model physics. In the current era of experimental technology it is probably only neutrinoless double beta decay ( $0\nu\beta\beta$ ), which has the ability to clarify the nature and provide the absolute effective mass of neutrinos. Observation of  $0\nu\beta\beta$  implies not only neutrinos are Majorana particles but also the lepton number violation. There are already intense activities going on over the world-wide for the experimental searches of  $0\nu\beta\beta$ . In these experiments, some are currently in their running phase and several experiments have been projected. With the same motivation as the other experiments, the TIN-TIN (The **IN**dia's **TIN** detector) experiment has been projected by the scientific community of India. This experiment, in coming future, will be housed in the approved underground laboratory of INO (India based Neutrino Observatory), to search  $0\nu\beta\beta$  using enriched  $^{124}\text{Sn}$  isotope as the target mass. In the present paper we have calculated the required sensitivity for  $^{124}\text{Sn}$  isotope in terms of exposure ( $\beta\beta_{\text{isotope}}$  mass  $\times$  time) and background rate (counts/ton-year-keV) at the projected FWHM energy resolution. Such that, after achieving the required sensitivity the TIN-TIN can really see the events of  $0\nu\beta\beta$  decay, if it exists in nature.

**PACS number(s):** 12.60.Fr, 11.15.Ex, 23.40-s, 14.60.Pq

**Keywords:** Double Beta Decay, Neutrino Mass and Mixing, Neutrino Mass Hierarchy.

# Quadratic magnetooptic spectroscopy setup based on photoelastic light modulation

Robin Silber<sup>1,2</sup>, Michaela Tomíčková<sup>1</sup>, Jari Rodewald<sup>3</sup>, Joachim Wollschläger<sup>3</sup>, Martin Veis<sup>4</sup>, Timo Kuschel<sup>2</sup>, Jaroslav Hamrle<sup>1,4</sup>

<sup>1</sup> Nanotechnology Centre, VSB-Technical University of Ostrava,  
17. listopadu 15, 70833 Ostrava, Czech Republic

<sup>2</sup> Center for Spinelectronic Materials and Devices, Department of Physics,  
Bielefeld University, Universitätsstraße 25, 33615 Bielefeld, Germany

<sup>3</sup> Department of Physics and Center of Physics and Chemistry of New Materials,  
Osnabrück University, 49076 Osnabrück, Germany

<sup>4</sup> Faculty of Mathematics and Physics, Charles University, Ke Karlovu 5, 12116 Prague, Czech Republic  
(Dated: February 14, 2018)

In most of the cases the magnetooptic Kerr effect (MOKE) techniques rely solely on the effects linear in magnetization ( $\mathbf{M}$ ). Nevertheless, a higher-order term being proportional to  $\mathbf{M}^2$  and called quadratic MOKE (QMOKE) can additionally contribute to experimental data. Handling and understanding the underlying origin of QMOKE could be the key to utilize this effect for investigation of antiferromagnetic materials in the future due to their vanishing first order MOKE contribution. Also, better understanding of QMOKE and hence better understanding of magnetooptic (MO) effects in general is very valuable, as the MO effect is very much employed in research of ferro- and ferrimagnetic materials. Therefore, we present our QMOKE and longitudinal MOKE spectroscopy setup with a spectral range of 0.8–5.5 eV. The setup is based on light modulation through a photoelastic modulator and detection of second-harmonic intensity by a lock-in amplifier. To measure the Kerr ellipticity an achromatic compensator is used within the setup, whereas without it Kerr rotation is measured. The separation of QMOKE spectra directly from the measured data is based on measurements with multiple magnetization directions. So far the QMOKE separation algorithm is developed and tested for but not limited to cubic (001) oriented samples. The QMOKE spectra yielded by our setup arise from two quadratic MO parameters  $G_s$  and  $2G_{44}$ , being elements of quadratic MO tensor  $\mathbf{G}$ , which describe perturbation of the permittivity tensor in the second order in  $\mathbf{M}$ .

## I. INTRODUCTION

The magnetooptic Kerr effect (MOKE)<sup>1</sup> technique is a tool that was and is vastly used for ferro- and ferrimagnetic material research. Setups employing MOKE at a single wavelength are typically used to provide information about magnetic properties of the sample such as magnetic anisotropy, magnetic remanence and coercivity, saturation field, magnetization ( $\mathbf{M}$ ) reversal process or detection of exchange bias. On the other hand, setups providing MOKE response over a continuous spectrum (usually extended visible spectral range) yield the information about the electronic structure of the sample (here the results are usually accompanied by ab-initio calculations).<sup>2–13</sup> Note that in both cases, one is usually relying on MOKE linear in  $\mathbf{M}$  (LinMOKE), while its contribution quadratic in  $\mathbf{M}$ , quadratic MOKE (QMOKE), is considered to be more of a parasitic effect. Nevertheless, the QMOKE effects are often accompanying LinMOKE measurements, and hence its clear understanding is important. Further, the fact that QMOKE is even in  $\mathbf{M}$  make it applicable for investigating antiferromagnetic materials which do not have a LinMOKE response.

At the beginning of the 90's unexpected symmetric contributions to the hysteresis loops of Ni-Fe bilayers were reported<sup>14,15</sup> and later on explained as QMOKE contributions to the overall MOKE signal.<sup>16–18</sup> Several methods have been proposed for the separation of QMOKE contributions from the LinMOKE signal

including the ROTMOKE method,<sup>19</sup> the 8-directional method,<sup>20</sup> the sample rotation by  $180^\circ$ ,<sup>21</sup> and the rotation field method.<sup>22</sup> Here we present QMOKE spectroscopy setup, which is capable to measure two types of QMOKE spectra in the spectral range of a 0.8–5.5 eV, QMOKE  $\sim G_s$  spectra and QMOKE  $\sim 2G_{44}$ , where  $G_s$  and  $2G_{44}$  are quadratic magnetooptic (MO) parameters that fully describe the perturbation to the permittivity tensor in the second order in  $\mathbf{M}$  of materials with cubic crystallographic structure.<sup>23–26</sup> LinMOKE spectra, namely longitudinal MOKE (LMOKE) spectra, can be measured as well. The measurement process is based on light modulation using photoelastic modulator and consequent detection by a lock-in amplifier. For the separation of LMOKE and of each QMOKE contribution, we employed a technique similar to the 8-directional method, but using a combination of just 4 directions and a sample rotation by  $45^\circ$  as described in this article.

## II. THEORY OF MOKE

### A. Description of polarized light and MOKE

MOKE manifests through the change of the polarization state of light reflected from a magnetized sample. Generally elliptically (fully) polarized light can be described by the Jones formalism using Jones vector such as<sup>27</sup>

# Experimental Implementation of a Large Scale Multipost Re-Entrant Array

Maxim Goryachev,<sup>1</sup> Jaemo Jeong,<sup>2</sup> and Michael E. Tobar<sup>1, a)</sup>

<sup>1)</sup>ARC Centre of Excellence for Engineered Quantum Systems, University of Western Australia, 35 Stirling Highway, Crawley WA 6009, Australia

<sup>2)</sup>Sungkyunkwan University, 25-2 Sungkyunkwan-ro, Myeongnyun 3(sam)ga, Jongno-gu, Seoul, South Korea

(Dated: 14 February 2018)

We demonstrate possibilities of a large scale multi-post re-entrant cavity with two case studies implemented with the same physical structure. The first demonstration implements two discrete Fabry-Pérot cavities crossing at the centre. The configuration allows the control not only of the resonance frequencies, but also a whole band gap and transmission band of frequencies between the directly excited diagonal and a higher frequency band. The second experiment demonstrates appearance of discrete Whispering Gallery Modes on a circle of re-entrant post. With the introduction of an artificial "scatterer", we demonstrate control over the doublet mode splitting.

Single post re-entrant cavities<sup>1,2</sup> have found numerous applications in many areas of engineering and physics. Among engineering applications, one may also consider material science and chemistry applications where these structures have been used to probe dielectric and magnetic properties of gases, liquids and solids<sup>3-6</sup>. Re-entrant cavities have become a de-factor standard component in accelerator physics<sup>7</sup>. Other applications include microwave transducers for gravity wave detectors<sup>8</sup> and dark matter detection<sup>9</sup>, hybrid quantum systems<sup>6</sup> and plasma-assisted combustion<sup>10</sup>.

A single post re-entrant cavity is a closed conducting structure with a metallic rod protruding from one cavity wall and leaving a small gap with the opposite one. The rod makes an equivalent inductance and the gap creates an equivalent capacitance. The resonance of these two quantities is highly tuneable with the gap size<sup>1,2</sup>. This can be done either mechanically through modifying the distance between the post and the opposite wall or electrically through changing electrical distance. Another advantage of this type of mode is that it depends mostly on the dimensions associated with the post rather than with the cavity enclosure, thus, this isolated mode can be adjusted to any frequency within the microwave and even the millimeterwave band.

A natural generalisation of the concept described above is a transition from a single re-entrant post to multiple posts within the same enclosure arranged in 1D<sup>11</sup> or 2D<sup>12</sup> structures with endless possibilities allowing the implementation of reconfigurable photonic topological insulators<sup>13</sup>. Within this approach each post represent a separate resonant element, a harmonic oscillator, coupled to others via magnetic field. Thus, the total number of re-entrant resonances equals to the number of posts. With such structures it is possible to manipulate not only eigenfrequencies of the structure but also field patterns to allow low and high concentration of magnetic fields in small regions that may be useful

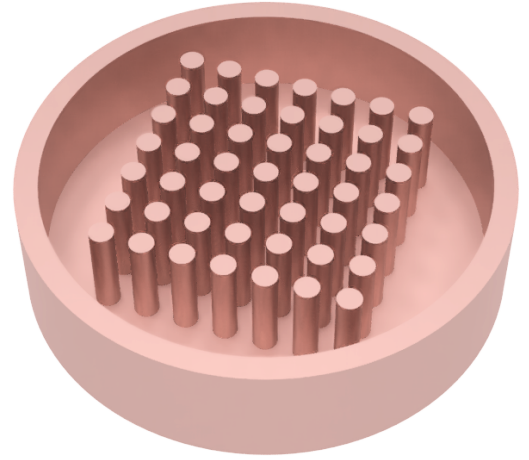


FIG. 1. 3D picture of a 49-post re-entrant cavity without the top lid.

for many applications<sup>6</sup>. Recently it was shown experimentally, that even with a large amount of resonators, finite element analysis could be implemented to understand complicated multiple-resonant structures.<sup>14</sup>

To demonstrate possibilities of large scale multi-post cavities experimentally, we implement a 7 by 7 regular square array of posts sharing the same walls as shown in Fig. 1. The cylindrical prototype with 58 mm diameter and 3.4 mm high is manufactured from copper for room temperature operation. Each post is made as a detached element with one threaded end to control the gap mechanically in the screw-like manner. This solution allows to roughly adjust or short-circuit re-entrant gaps for each post individually or remove each post completely giving us 49 independent degrees of freedom. Each post is 2.5 mm in diameter with 5 mm spacing between centres of adjacent elements.

The cavity is exited and probed via two loop microwave probes located at the vertices of the array. The device is characterised at room temperature with a Vector Network Analyser measuring its transmission from one port to another from 10 MHz to 18 GHz. Observed modes

<sup>a)</sup>Electronic mail: michael.tobar@uwa.edu.au



International Journal of Modern Physics A  
© World Scientific Publishing Company

## Potentialities of the future technical improvements in the search of rare nuclear decays by bolometers

Fabio Bellini

*Sapienza Università di Roma, P.le Aldo Moro 2 Roma, 00185, Italy*

*INFN, Sezione di Roma, P.le Aldo Moro 2, 00185, Rome, Italy*  
*fabio.bellini@roma1.infn.it*

Received Day Month Year

Revised Day Month Year

Bolometers are cryogenic calorimeters which feature excellent energy resolution, low energy threshold, high detection efficiency, flexibility in choice of materials, particle identification capability if operated as hybrid devices. After thirty years of rapid progresses, they represent nowadays a leading technology in several fields: particle and nuclear physics, X-ray astrophysics, cosmology. However, further and substantial developments are required to increase the sensitivity to the levels envisioned by future researches. A review of the challenges to be addressed and potentialities of bolometers in the search for rare nuclear decays is given, with particular emphasis to the neutrinoless double beta decay physics case.

*Keywords:* Low Temperature Detectors; Bolometers; Double Beta Decay; Rare Nuclear Decay

PACS numbers: 07.20.Mc, 23.40.-s, 23.60.+e, 14.60.Pq

### Contents

1. Introduction . . . . .	2
2. High Energy Resolution Calorimeters . . . . .	3
2.1. Conventional Calorimeters . . . . .	3
2.2. Bolometers . . . . .	3
2.2.1. Strenghts and Weaknesses . . . . .	5
2.2.2. Hybryd bolometers . . . . .	6
3. Double Beta Decay . . . . .	6
3.1. The $0\nu\beta\beta$ physics case . . . . .	6
3.2. Other second order weak processes . . . . .	8
4. Bolometers with Active Background Suppression . . . . .	9
4.1. Scintillating bolometers . . . . .	9
4.2. Cherenkov light in $\text{TeO}_2$ bolometers . . . . .	12
4.2.1. Transition edge sensors and metallic magnetic calorimeters . . . . .	13



# Future Ground-based Wide Field of View Air Shower Detectors

Di Sciascio Giuseppe\*

INFN - Roma Tor Vergata

E-mail: [disciascio@roma2.infn.it](mailto:disciascio@roma2.infn.it)

Extensive air shower (EAS) arrays directly sample the shower particles that reach the observation altitude. They are wide field of view (FoV) detectors able to view the whole sky simultaneously and continuously. In fact, EAS arrays have an effective FoV of about 2 sr and operate with a duty cycle of  $\sim 100\%$ . This capability makes them well suited to study extended sources, such as the Galactic diffuse emission and measure the spectra of Galactic sources at the highest energies (near or beyond 100 TeV). Their sensitivity in the sub-TeV/TeV energy domain cannot compete with that of Cherenkov telescopes, but the wide FoV is ideal to perform unbiased sky surveys, discover transients or explosive events (GRBs) and monitor variable or flaring sources such as Active Galactic Nuclei (AGN). An EAS array is able to detect at the same time events induced by photons and charged cosmic rays, thus studying the connection between these two messengers of the non-thermal Universe. Therefore, these detectors are, by definition, multi-messenger instruments.

Wide FoV telescopes are crucial for a multi-messenger study of the Gravitational Wave events due to their capability to survey simultaneously all the large sky regions identified by LIGO and VIRGO, looking for a possible correlated  $\gamma$ -ray emission.

In this contribution we summarize the scientific motivations which push the construction of new wide FoV air shower detectors and introduce the future instruments currently under installation. Finally, we emphasize the need of an EAS array in the Southern hemisphere to monitor the Inner Galaxy and face a number of important open problems.

XII Multifrequency Behaviour of High Energy Cosmic Sources Workshop

12-17 June, 2017

Palermo, Italy

\*Speaker.

© Copyright owned by the author(s) under the terms of the Creative Commons Attribution-NonCommercial-NoDerivatives 4.0 International License (CC BY-NC-ND 4.0).

<https://pos.sissa.it/>

Wide Field of View Detectors

Di Sciascio Giuseppe

## 1. Open problems in Cosmic Ray Physics

Understanding the origin of the "knee" in the energy spectrum of the primary radiation is the key for a comprehensive theory of the origin of Cosmic Rays (hereafter CR) up to the highest observed energies. In fact, the knee is clearly connected with the issue of the end of the Galactic CR spectrum and the transition from Galactic to extra-galactic CRs.

If the knee, a steepening of the spectral index from  $\sim -2.7$  to  $\sim -3.1$  at about 3 PeV ( $\approx 3 \times 10^{15}$  eV), is a source property we should see a corresponding spectral feature in the gamma-ray spectra of the CR sources. If, on the contrary, this feature is the result of propagation, we should observe a knee that is potentially dependent on location, because the propagation properties depend, in principle, on the position in the Galaxy.

To understand the origin of the knee we need to deepen our understanding of acceleration, escape and propagation of the relativistic particles, the main pillars that constitute the SuperNova paradigm for the origin of the radiation (see [1] and references therein). We need to identify the sources and the mechanisms able to accelerate particles beyond PeV energies (the so-called "PeVatrons"). We need to understand how particles escape from the sources and are released into the interstellar medium. Finally, we need to understand how particles propagate through the Galaxy before reaching the Earth.

It is widely believed that the bulk of CRs up to about  $10^{17}$  eV are Galactic, produced and accelerated by the shock waves of SuperNova Remnants (SNR) expanding shells [2]. The SNR paradigm has two bases: firstly, the energy released in SN explosions can explain the CR energy density considering an overall efficiency of conversion of explosion energy into CR particles of the order of 10%. Secondly, the diffusive shock acceleration operating in SNR can provide the necessary power-law spectral shape of accelerated particles with spectral index  $-2.0$  that subsequently steepen to  $-2.7$ , as observed, due to the energy-dependent diffusive propagation effect (see [3] and references therein).

SuperNovae are believed to be almost the only available power source. However, recent claims by H.E.S.S. of a possible detection of a PeVatrons in the Galactic Center, most likely related to a supermassive black hole [4], opens new perspectives showing that galactic PeVatrons other than SNRs may exist.

Recently AGILE and Fermi observed GeV photons from two young SNRs (W44 and IC443) showing the typical spectrum feature around 1 GeV (the so-called ' $\pi^0$  bump', due to the decay of  $\pi^0 \rightarrow \gamma\gamma$ ) related to hadronic interactions [5, 6]. This important measurement, however, does not demonstrate the capability of SNRs to produce the power needed to maintain the galactic CR population and to accelerate CRs up to the knee, at least. In fact, unlike neutrinos that are produced only in hadronic interactions, the question whether  $\gamma$ -rays are produced by the decay of  $\pi^0$  from protons or nuclei interactions ('hadronic' mechanism), or by a population of relativistic electrons via Inverse Compton scattering or bremsstrahlung ('leptonic' mechanism), still needs a conclusive answer.

One of the main open problems in the SNR origin model is the maximum energy that can be attained by a CR particle in SNR. To accelerate protons up to the PeV energy domain a significant amplification of the magnetic field at the shock is required but this process is problematic in SNRs [7]. However, if the knee is a propagation effect, the Galaxy could contain "super-PeVatrons",

# How blind are underground and surface detectors to strongly interacting Dark Matter?

Timon Emken\* and Chris Kouvaris†

*CP3-Origins, University of Southern Denmark, Campusvej 55, DK-5230 Odense, Denmark*

(Dated: February 14, 2018)

Above a critical dark matter-nucleus scattering cross section any terrestrial direct detection experiment loses sensitivity to dark matter, since the Earth crust, atmosphere, and potential shielding layers start to block off the dark matter particles. This critical cross section is commonly determined by describing the average energy loss of the dark matter particles analytically. However, this treatment overestimates the stopping power of the Earth crust. Therefore the obtained bounds should be considered as conservative. We perform Monte Carlo simulations to determine the precise value of the critical cross section for various direct detection experiments and compare them to other dark matter constraints in the low mass regime. In this region we find parameter space where typical underground and surface detectors are completely blind to dark matter. This “hole” in the parameter space can hardly be closed with an increase in the detector exposure. Dedicated surface or high-altitude experiments may be the only way to directly probe this part of the parameter space.

## I. INTRODUCTION

The existence of large quantities of dark matter (DM) in the universe is backed by strong astrophysical evidence [1, 2]. Direct detection experiments are consequently trying to observe non-gravitational interactions between DM particles from the galactic halo and target atoms inside a terrestrial detector [3, 4]. So far no conclusive signal has been reported, and detectors continue probing weaker and weaker DM-nucleon interactions by increasing their exposure [5] or extend their search to lower DM masses by decreasing their recoil energy threshold [6, 7]. Other approaches focus on experimental signals other than nuclear recoils to probe light DM, as e.g. DM-electron scatterings [8] or inelastic DM-atom scatterings that produce photons [9, 10].

These experiments are typically located underground, beneath  $\sim 1$  km of rock, and equipped with additional shielding layers in order to reduce background signals. This comes at the price of impairing the experiment’s sensitivity to strongly interacting DM, since elastic DM-nucleus collisions occur not only in the target material but also inside the Earth crust prior to reaching the detector. These collisions slow down and deflect the DM, attenuating the flux of DM particles capable of triggering the detector, such that the Earth crust could shield off DM. Above a critical cross section the shielding effect of the crust or the atmosphere is effective enough that any detector on Earth becomes blind.

The scenario of strongly interacting DM<sup>1</sup> is highly constrained by astrophysical observations. Strong interactions between DM and baryons in the early universe lead to momentum transfer between them and alter the anisotropy of the Cosmic Microwave background (CMB) [11–13]. Strong interactions between DM and cosmic ray nuclei lead to the production of neutral pions and consequently  $\gamma$ -rays [14–16]. They also introduce a collisional damping effect during cosmological structure formation [17]. Further constraints on

strongly interacting DM are set by satellite experiments such as IMP7/8 [18, 19], early experiments on the Skylab space station [19, 20], the rocket-based X-ray Quantum Calorimeter experiment (XQC) [21], as well as balloon-based experiments such as IMAX [19, 22] and the one by Rich et al [23]. Considering that terrestrial detectors lose sensitivity above a certain cross section, an important question is whether or not there exists allowed parameter space, a “window” between the constraints mentioned above and the ones from direct detection [24].

Indeed there have been several allowed windows in the constraints on strongly interacting DM over a wide range of DM masses [24, 25]. In order to close these windows, new constraints were derived based on DM capture and heat flow inside the Earth [26], on observations by the IceCube experiment [27] and the Fermi Gamma-ray Space Telescope [15]. For light DM a window in the constraints was closed by re-analyzing old results from DAMIC and XQC [28], and using the new results of the CRESST 2017 surface run [29]. Most recently several holes in the constraints on super-heavy DM were closed using direct detection experiments only, namely by a re-analysis of CDMS-I [30].

As we mentioned, pre-detection DM-nuclei scatterings can reduce and effectively eliminate the flux of detectable DM particles in underground detectors. Consequently terrestrial experiments constrain DM-nucleon cross section within a band only. Below the lower limit, there is simply not enough exposure for an experiment to probe DM. Above the upper critical cross section, no constraint can be imposed, because DM interacts too strongly with nuclei and loses enough energy or gets deflected, resulting in a non-detectable flux at the location of the detector.

In this paper, we use Monte Carlo (MC) techniques to precisely determine this upper critical cross section, above which each experiment fails to probe DM. Previous works on this matter treated the stopping of DM in an overburden with analytic formulae which capture the average energy loss of DM particles traversing through the Earth crust [24, 29–31]. However, this analytic treatment does not suffice for a precise determination of the critical cross section. Since the analytic description overestimates the stopping power of the Earth crust by capturing the average energy loss, the bounds obtained this

\* E-mail: emken@cp3.sdu.dk

† E-mail: kouvaris@cp3.sdu.dk

<sup>1</sup> We emphasize that strongly interacting DM refers to DM-nucleon interactions and not DM self-interactions.

# Exclusive vector meson photoproduction in fixed - target collisions at the LHC

V. P. Gonçalves and M. M. Jaime

*High and Medium Energy Group,  
Instituto de Física e Matemática,  
Universidade Federal de Pelotas*

*Caixa Postal 354, CEP 96010-900, Pelotas, RS, Brazil*

(Dated: February 14, 2018)

The exclusive  $\rho$ ,  $\omega$  and  $J/\Psi$  photoproduction in fixed - target collisions at the LHC is investigated. We estimate, for the first time, the rapidity and transverse momentum distributions of the vector meson photoproduction in  $pHe$ ,  $pAr$ ,  $PbHe$  and  $PbAr$  fixed - target collisions at the LHC using the STARlight Monte Carlo and present our results for the total cross sections. Predictions taken into account the kinematical range probed by the LHCb detector are also presented. Our results indicate that the experimental analysis of this process in fixed - target collisions at the LHC is feasible, which allows to probe the QCD dynamics in a kinematical range complementary to that studied in the collider mode.

PACS numbers: 12.38.-t; 13.60.Le; 13.60.Hb

Keywords: Ultraperipheral Heavy Ion Collisions, Vector Meson Production, Fixed - target collisions

The Large Hadron Collider (LHC) at CERN started high energy collisions ten years ago. During this period a large amount of data have been collected considering  $pp$  collisions at  $\sqrt{s} = 0.9, 2.76, 7, 8$  and  $13$  TeV,  $pPb$  collisions at  $\sqrt{s} = 5$  and  $8.2$  TeV as well as  $PbPb$  collisions at  $\sqrt{s} = 2.76$  and  $5$  TeV. Currently, there is a great expectation that LHC will discover new physics beyond the Standard Model, such as supersymmetry or extra dimensions. However, we should remember that one of the main contributions of the LHC is that it probes a new kinematical regime at high energy, where several questions related to the description of the Quantum Chromodynamics (QCD) remain without satisfactory answers. In particular, the study of the photon - induced interactions in hadronic collisions at the LHC [1, 2] is expected to constrain the nuclear and nucleon gluon distributions [3] and the description of the QCD dynamics at high energies [4], where a hadron becomes a dense system and the nonlinear effects inherent to the QCD dynamics may become visible [5]. During the last years, the study of these interactions in  $pp/pA/AA$  collisions [1] became a reality [6–14] and new data associated to the Run 2 of the LHC are expected to be released soon.

A complementary kinematical range can be studied in fixed - target collisions at the LHC. Such alternative, proposed originally in Ref. [15], is expected to probe for example the nucleon and nuclear matter in the domain of high Feynman  $x_F$ , the transverse spin asymmetries in the Drell - Yan and Quarkonium production as well as the Quark Gluon Plasma formation in the energy and density range between the SPS and RHIC experiments [16]. The basic idea of the AFTER@LHC experiment is to develop a fixed - target programme using the proton and heavy ions beams of the LHC, extracted by a bent crystal, to collide with a fixed proton or nuclear target, reaching high luminosities when a target with a high density is considered. The typical energies that are expected to be reached in this experiment are  $\sqrt{s} \approx 110$  GeV for  $pA$  collisions and  $\sqrt{s} \approx 70$  GeV for  $PbA$  collisions.

Very recently, the study of fixed - target collisions at the LHC became a reality by the injection of noble gases ( $He$ ,  $Ne$ ,  $Ar$ ) in the LHC beam pipe by the LHCb Collaboration [17] using the System for Measuring Overlap with Gas (SMOG) device [18]. The typical fixed - target  $pA$  and  $PbA$  configurations that already have been performed were  $pAr$  collisions at  $\sqrt{s} = 69$  GeV,  $pNe$  at  $\sqrt{s} = 87$  GeV,  $pHe/pNe/pAr$  at  $\sqrt{s} = 110$  GeV,  $PbNe$  at  $\sqrt{s} = 54$  GeV and  $PbAr$  at  $\sqrt{s} = 69$  GeV. The associated experimental results are expected to improve our understanding of the nuclear effects present in  $pA$  collisions [19] and, in the particular case of  $pHe$  collisions, to shed light on the antiproton production (See e.g. Ref. [20]).

The study of photon - induced interactions also is expected to be possible in fixed - target collisions [15]. As demonstrated in Refs. [21, 22], the analysis of the exclusive dilepton and  $\eta_c$  photoproduction in ultraperipheral collisions at AFTER@LHC can be useful to probe the inner hadronic structure and the existence of the Odderon, which is one the main open questions of the strong interactions theory [23]. Assuming  $\sqrt{s} = 115/72/72$  GeV for  $pp/Pbp/PbPb$  collisions, one have that the typical values for the maximum photon - hadron and photon - photon center - of - mass energies are  $\sqrt{s_{\gamma h}} \lesssim 44/12/9$  GeV and  $\sqrt{s_{\gamma\gamma}} \lesssim 17/2.0/1.0$  GeV, respectively. Therefore, the fixed - target collisions allows to probe the photon - induced interactions in a limited energy range, dominated by low - energy interactions. Such analysis can be considered as complementary to those performed in the collider mode, where the maximum energies can reach values of  $\mathcal{O}(TeV)$  and the cross sections receive contributions of low and high energies  $\gamma\gamma$  and  $\gamma h$  interactions [1].

In this paper we will study, by the first time, the exclusive vector meson photoproduction in fixed - target collisions. In particular, we will estimate the rapidity and transverse momentum distributions for the exclusive  $\rho$ ,  $\omega$  and  $J/\Psi$  photoproduction in  $pA$  and  $PbA$  collisions at the energies and configurations considered by

# Higgs Pair Production at Future Hadron Colliders: From Kinematics to Dynamics

Dorival Gonçalves,<sup>1</sup> Tao Han,<sup>1</sup> Felix Kling,<sup>2</sup> Tilman Plehn,<sup>3</sup> and Michihisa Takeuchi<sup>4</sup>

<sup>1</sup>*PITT PACC, Department of Physics and Astronomy, University of Pittsburgh, USA*

<sup>2</sup>*Department of Physics and Astronomy, University of California, Irvine, USA*

<sup>3</sup>*Institut für Theoretische Physik, Universität Heidelberg, Germany*

<sup>4</sup>*Kavli IPMU (WPI), UTIAS, University of Tokyo, Kashiwa, Japan*

The measurement of the triple Higgs coupling is a key benchmark for the LHC and future colliders. It directly probes the Higgs potential and its fundamental properties in connection to new physics beyond the Standard Model. There exist two phase space regions with an enhanced sensitivity to the Higgs self-coupling, the Higgs pair production threshold and an intermediate top pair threshold. We show how the invariant mass distribution of the Higgs pair offers a systematic way to extract the Higgs self-coupling, focusing on the leading channel  $pp \rightarrow hh \rightarrow b\bar{b} \gamma\gamma + X$ . We utilize new features of the signal events at higher energies and estimate the potential of a high-energy upgrade of the LHC and a future hadron collider with realistic simulations. We find that the high-energy upgrade of the LHC to 27 TeV would have the potential to reach 30% accuracy to measure the SM Higgs self-coupling and a future 100 TeV collider could improve the measurement to better than 10%.

## CONTENTS

I. Introduction	1
II. Higgs Pair Signature	2
III. The Mother of Distributions	3
IV. Detector-level Analysis	5
V. Summary and Outlook	7
References	9

## I. INTRODUCTION

The discovery of the Higgs boson [1, 2] at the CERN Large Hadron Collider (LHC) is of monumental significance. The completion of the Standard Model (SM) provides us with a consistent theory valid up to high scales. As a perturbative gauge theory, it allows for precision predictions for essentially all LHC observables. In parallel, experimental advances have turned ATLAS and CMS into the first hadron collider precision experiments in history. In combination, these developments open new avenues to tackle fundamental physics questions at the LHC and future high-energy facilities.

On the theory side, we are still lacking an understanding if and how the Higgs mass, the only dimensionful parameter in the theory, is stabilized against a large new physics scale. The Higgs potential responsible for the electroweak symmetry breaking (EWSB) in the SM is determined by the triple and quartic Higgs self-coupling  $\lambda_{\text{SM}} \approx 1/8$ . It is a true self-interaction in the sense that it is not associated with any conserved charge after EWSB. With our ignorance for new physics beyond the SM, the shape of the Higgs potential is deeply linked to the fundamental question of electroweak symmetry breaking in the early universe, allowing for a slow second-order phase

transition in the SM or a strong first-order phase transition with a modified Higgs potential. It has been argued that a wide range of modified Higgs potentials, which result in a strong first-order EW phase transition, lead to order-one modifications of  $\lambda_{\text{SM}}$  [3]. All of this points to the Higgs self-coupling  $\lambda$  as a benchmark measurement for the coming LHC runs, as well as any kind of planned colliders [4].

Higgs pair production  $pp \rightarrow hh$  offers a direct path to pin down  $\lambda$  at a hadron collider [5, 6]. Previous studies show that promising final states from the  $hh$  decays are  $b\bar{b}\gamma\gamma$  [7, 8],  $b\bar{b}\tau\tau$  [9, 10],  $b\bar{b}WW$  [11],  $b\bar{b}b\bar{b}$  [12], and  $4W$  [13]. Theoretical studies as well as current analyses point to the  $b\bar{b}\gamma\gamma$  decay as the most promising signature at the LHC [14]. Combinations with indirect measurements of the self-coupling from quantum effects confirm that Higgs pair production provides the most robust self-coupling measurement [15]. For the high-luminosity LHC (HL-LHC), ATLAS and CMS projections indicate a very modest sensitivity to the Higgs self-coupling [16].

In anticipation to probe new physics beyond the SM, it is customary to parametrize the modification of the self-coupling as

$$\kappa_\lambda = \frac{\lambda}{\lambda_{\text{SM}}} . \quad (1)$$

In the optimistic scenario that we can neglect systematic uncertainties, those studies indicate that the LHC will probe the coupling at 95% confidence level

$$-0.8 < \kappa_\lambda < 7.7 . \quad (2)$$

An issue with those studies is that they are based on the total rate for Higgs production, but neglect a wealth of available information. Including a full kinematic analysis could lead to an improved measurement [17]

$$-0.2 < \kappa_\lambda < 2.6 , \quad (3)$$

# Future Deep Inelastic Scattering with the LHeC

Max Klein (University of Liverpool)

Contribution to a Book dedicated to the Memory of Guido Altarelli, January 21, 2018

## Abstract

For nearly a decade, Guido Altarelli accompanied the Large Hadron electron Collider project, as invited speaker, referee and member of the International Advisory Committee. This text summarises the status and prospects of the development of the LHeC, with admiration for a one-time scientist and singular leader whom I met first nearly 40 years ago under the sun shining for the “Herceg Novi School” in Kupari, where we both lectured about the beautiful science of Deep Inelastic Scattering and enjoyed life under a yellow moon.

## 1 Introduction

The time is now 50 years after the birth of deep inelastic scattering (DIS) with the discovery of partons [1, 2] and 40 years after the paper of Altarelli and Parisi, cited over six thousand times, on “Asymptotic Freedom in Parton Language” [3]. We are 20 years after the approval of the huge LHC detectors, ATLAS and CMS. These have now taken about  $100\text{ fb}^{-1}$  of data each. Adding the publications of all LHC collaborations, nearly two thousand papers have appeared, based on the superb performance of the Large Hadron Collider. The Higgs boson was discovered five years ago. About this most impressive harvest Guido Altarelli had noted, *we expected complexity but we found a maximum of simplicity* [4], commenting not on the hugely complex experiments nor ingenuitive, novel analysis techniques but referring to the surprising absence of new physics, besides the exciting observation of the Higgs boson. No evidence was observed so far in support for extra dimensions, symmetries, particles nor a grand unified theory. Guido thought about this deeply: *..it is true that the SM theory is renormalizable and completely finite and predictive. If you forget the required miraculous fine tuning you are not punished, you find no catastrophe! .. The possibility that the Standard Model holds well beyond the electroweak scale must now be seriously considered.. We are experiencing a very puzzling situation but, to some extent, this is good because big steps forward in fundamental physics have often originated from paradoxes. We highly hope that the continuation of the LHC experiments will bring new light on these problems...* [4].

The LHC is now projected to operate for two decades hence, with a major interrupt for accelerator and detector upgrades in between. A new horizon for these explorations would be opened with an additional  $ep/eA$  experiment, i.e. with electron-proton (and electron-ion) collisions concurrent to the default LHC operation in the thirties. The Large Hadron electron Collider (LHeC) was principally designed in an extended concept report (CDR) [5]. This was published in June 2012, a few weeks before the Higgs boson discovery was announced. It considers the addition to the LHC of a 60 GeV energy electron beam accelerator, arranged tangential to the main ring of 27 km circumference. This configuration is thought to form a novel  $ep$  and  $eA$  experiment which would be able to collect  $O(1)\text{ ab}^{-1}$  of integrated luminosity, exceeding the HERA result by a factor of thousand and its kinematic range by nearly 20. Its salient feature will be the synchronous operation of  $ep$  with  $pp$  such that no principal loss of LHC luminosity shall occur. The LHeC would enable electron-hadron energy frontier physics explorations at about 1 TeV cms energy, which is four times higher than future Higgs facilities, such as in China (CepC) or Japan (ILC), may achieve in electron-positron collisions. The question such a programme of deep inelastic electron-hadron scattering at the LHC has to answer consists of how that may lead to new insight into the SM and beyond, on its own and in complementing the  $pp$  and heavy ion physics pursued at the Large Hadron Collider. This paper has

# Discriminating WIMP–nucleus response functions in present and future XENON-like direct detection experiments

A. Fieguth,<sup>1,\*</sup> M. Hoferichter,<sup>2,†</sup> P. Klos,<sup>3,4,‡</sup> J. Menéndez,<sup>5,§</sup> A. Schwenk,<sup>3,4,6,¶</sup> and C. Weinheimer<sup>1,\*\*</sup>

<sup>1</sup>*Institut für Kernphysik, Westfälische Wilhelms-Universität Münster, 48149 Münster, Germany*

<sup>2</sup>*Institute for Nuclear Theory, University of Washington, Seattle, WA 98195-1550, USA*

<sup>3</sup>*Institut für Kernphysik, Technische Universität Darmstadt, 64289 Darmstadt, Germany*

<sup>4</sup>*ExtreMe Matter Institute EMMI, GSI Helmholtzzentrum für Schwerionenforschung GmbH, 64291 Darmstadt, Germany*

<sup>5</sup>*Center for Nuclear Study, The University of Tokyo, 113-0033 Tokyo, Japan*

<sup>6</sup>*Max-Planck-Institut für Kernphysik, Saupfercheckweg 1, 69117 Heidelberg, Germany*

The standard interpretation of direct-detection limits on dark matter involves particular assumptions of the underlying WIMP–nucleus interaction, such as, in the simplest case, the choice of a Helm form factor that phenomenologically describes an isoscalar spin-independent interaction. In general, the interaction of dark matter with the target nuclei may well proceed via different mechanisms, which would lead to a different shape of the corresponding nuclear structure factors as a function of the momentum transfer  $q$ . We study to what extent different WIMP–nucleus responses can be differentiated based on the  $q$ -dependence of their structure factors (or “form factors”). We assume an overall strength of the interaction consistent with present spin-independent limits and consider an exposure corresponding to XENON1T-like, XENONnT-like, and DARWIN-like direct detection experiments. We find that, as long as the interaction strength does not lie too much below current limits, the DARWIN settings allow a conclusive discrimination of many different response functions based on their  $q$ -dependence, with immediate consequences for elucidating the nature of dark matter.

## I. INTRODUCTION

The search for weakly interacting massive particles (WIMPs) as candidates for dark matter is pursued with increasing effort in direct detection experiments [1] that aim to observe hints for WIMPs scattering off target nuclei, see, e.g., [2–9] for recent limits. Among the available technologies, dual-phase xenon time projection chamber (TPC) detectors lead the search for WIMP masses  $m_\chi \gtrsim 5$  GeV [7–9]. The third generation experiment XENON1T presented first results from 34.2 live days utilizing  $\sim 1$  t fiducial mass [9], and is taking further data in order to achieve its projected sensitivity of a single-nucleon cross section of  $\sigma_0 = 1.6 \times 10^{-47}$  cm<sup>2</sup> for a WIMP mass  $m_\chi = 50$  GeV after an exposure of 2 ton years [10]. Ongoing efforts are expected to push sensitivities further in the next years, including the LZ detector [11], PandaX-xT [12], and an upgrade of XENON1T to the XENONnT experiment, with a planned active mass about three times larger [10]. On a longer time scale, the proposed DARWIN experiment [13] aims to cover the full parameter space before the coherent neutrino–nucleus scattering [14] becomes the dominant background.

Traditionally, experimental analyses assume a standard isoscalar spin-independent (SI) interaction between the WIMP and the xenon nuclei, with the underlying nu-

clear structure factor (also referred to as “form factor”) approximated by a so-called Helm form factor [15]. This choice is motivated by the fact that if the standard SI isoscalar WIMP–nucleon interaction is present and not suppressed, it is expected to be the dominating contribution given the coherent enhancement by all  $A$  nucleons in a target nucleus. The differential WIMP scattering rate per unit energy

$$\frac{dR}{dE} \propto \frac{d\sigma}{dq^2} \propto \sigma_0 \times |\mathcal{F}(q^2)|^2, \quad (1)$$

is proportional to the product of the WIMP–nucleon cross section  $\sigma_0$  and the nuclear structure factor  $\mathcal{F}$  (normalized by  $\mathcal{F}(0) = A$  for the standard SI response). The momentum transfer  $q$  is related to the recoil energy  $E$  and the mass of the xenon nucleus  $m_A$  by  $E = q^2/2m_A$ . The limits derived from experimental analyses are usually presented in terms of the WIMP–nucleon cross section  $\sigma_0$ . However, Eq. (1) shows that the limit deduced on  $\sigma_0$  for a given differential WIMP recoil spectrum depends on the shape of  $\mathcal{F}$  as well as on its normalization. In particular, the standard limits on  $\sigma_0$  are valid only if the SI interaction is indeed the dominating contribution to WIMP–nucleus scattering.

However, if the isoscalar SI interaction is suppressed, e.g., in the vicinity of so-called blind spots in supersymmetric models [16–18], other channels become important and can even be dominant. This issue has been addressed experimentally by dedicated searches of alternative channels, e.g., those based on spin-dependent (SD) WIMP–nucleus interactions [19–22], non-relativistic effective field theory (NREFT) operators [23, 24], or generically  $q$ -suppressed responses [25]. More generally, the dynamics of the underlying strong interaction, quantum

\*E-mail: a.fieguth@uni-muenster.de

†E-mail: mhofer@uw.edu

‡E-mail: pklos@theorie.ikp.physik.tu-darmstadt.de

§E-mail: menendez@cns.s.u-tokyo.ac.jp

¶E-mail: schwenk@physik.tu-darmstadt.de

\*\*E-mail: weinheimer@uni-muenster.de

# Neutrino Predictions from Generalized CP Symmetries of Charged Leptons

Peng Chen,<sup>1,\*</sup> Salvador Centelles Chuliá,<sup>2,†</sup> Gui-Jun  
Ding,<sup>3,‡</sup> Rahul Srivastava,<sup>2,§</sup> and José W. F. Valle<sup>2,¶</sup>

<sup>1</sup>*College of Information Science and Engineering,  
Ocean University of China, Qingdao 266100, China*

<sup>2</sup>*AHEP Group, Institut de Física Corpuscular –  
C.S.I.C./Universitat de València, Parc Científic de Paterna.*

*C/ Catedrático José Beltrán, 2 E-46980 Paterna (Valencia) - SPAIN*

<sup>3</sup>*Interdisciplinary Center for Theoretical Study and Department of Modern Physics,  
University of Science and Technology of China, Hefei, Anhui 230026, China*

We study the implications of generalized CP transformations acting on the mass matrices of charged leptons in a model-independent way. Generalized  $e-\mu$ ,  $e-\tau$  and  $\mu-\tau$  symmetries are considered in detail. In all cases the physical parameters of the lepton mixing matrix, three mixing angles, and three CP phases, can be expressed in terms of a restricted set of independent “theory” parameters that characterize a given choice of CP transformation. This leads to implications for neutrino oscillations as well as neutrinoless double beta decay experiments.

PACS numbers: 14.60.Pq, 11.30.Er

---

\* pche@mail.ustc.edu.cn

† salcen@ific.uv.es

‡ dinggj@ustc.edu.cn

§ rahulsri@ific.uv.es

¶ valle@ific.uv.es



# Third Family Quark-Lepton Unification at the TeV Scale

Admir Greljo<sup>1,2,\*</sup> and Ben A. Stefanek<sup>1,†</sup>

<sup>1</sup>*PRISMA Cluster of Excellence & Mainz Institute for Theoretical Physics, Johannes Gutenberg-Universität Mainz, 55099 Mainz, Germany*

<sup>2</sup>*Faculty of Science, University of Sarajevo, Zmaja od Bosne 33-35, 71000 Sarajevo, Bosnia and Herzegovina*

We construct a model of quark-lepton unification at the TeV scale based on an  $SU(4)$  gauge symmetry, while still having acceptable neutrino masses and enough suppression in flavor changing neutral currents. An approximate  $U(2)$  flavor symmetry is an artifact of family-dependent gauge charges leading to a natural realization of the CKM mixing matrix. The model predicts sizeable violation of PMNS unitarity as well as a gauge vector leptoquark  $U_1^\mu = (\mathbf{3}, \mathbf{1}, 2/3)$  which can be produced at the LHC – both effects within the reach of future measurements. In addition, recently reported experimental anomalies in semi-leptonic  $B$ -meson decays, both in charged  $b \rightarrow c\tau\nu$  and neutral  $b \rightarrow s\mu\mu$  currents, can be accommodated.

## I. INTRODUCTION

Quark-lepton unification – as originally suggested by Jogesh Pati and Abdus Salam [1] – is an attractive paradigm of physics beyond the Standard Model (SM). Namely, a fundamental representation of an  $SU(4)$  gauge symmetry embeds a color triplet quark and a color singlet lepton ( $\mathbf{4} = \mathbf{3} \oplus \mathbf{1}$ ). Such a construction predicts existence of an exotic particle, a gauge vector leptoquark (LQ)  $U_1^\mu = (\mathbf{3}, \mathbf{1}, 2/3)$ , which can turn a quark into a lepton and vice versa.

In this article, we entertain the possibility of quark-lepton unification at the TeV scale, motivated by the scope of present particle laboratories. The two main challenges to this idea are (i) the observed neutrino masses and (ii) the stringent constraints from flavor changing neutral currents (FCNC) in meson decays. In particular, the neutrino masses are expected to be similar in size to the masses of the up-type quarks, since the two fields are embedded in the same  $\mathbf{4}$  of  $SU(4)$ . The correct structure for a solution comes naturally in high-scale Pati-Salam models, possibly in the context of  $SO(10)$  grand unification (GUT) [2], where the Majorana mass is around the GUT scale, while the Dirac mass is at the electroweak scale, leading to a seesaw mechanism [3–6]. On the contrary, quark-lepton unification at scales much lower than the GUT scale (but still far beyond LHC reach) was achieved in Ref. [7] using the *inverse seesaw mechanism* (ISS) [8–10] to generate small neutrino masses.

Also problematic for Pati-Salam quark-lepton unification at the TeV scale are the stringent bounds on FCNC in semi-leptonic meson decays (e.g.  $K_L \rightarrow \mu e$ ) due to gauge vector LQ exchange, pushing the LQ mass to the PeV ballpark [11–15]. On the other hand, as shown recently in Ref. [16], the FCNC induced by a TeV scale vector LQ can be avoided in the context of *partial unification* models [17, 18] in

which the SM gauge group is embedded into a larger  $SU(4) \times SU(3)' \times SU(2)_L \times U(1)'$  group (“4321”), and the (would-be) SM fermions are charged only under the “321” part. The LQ couplings to SM fermions are generated via mass mixing with extra vector-like fermions charged under  $SU(4)$ , where the largest LQ interactions are taken to be with the third family fermions as allowed by the low energy flavor data. Note that this construction does not have a neutrino mass problem since the (would-be) SM quarks and leptons are not unified in  $\mathbf{4}$  of  $SU(4)$ .<sup>1</sup>

Building on this work, the authors of Ref. [29] introduce family-dependent gauge interactions – Pati-Salam for every family ( $PS^3$ ) – achieving a TeV scale vector LQ dominantly coupled to the third family while still having quarks and leptons unified into a  $\mathbf{4}$  of  $SU(4)$ . Scalar link fields are introduced to break the gauge symmetry down to the SM. This is done in several steps with very hierarchical vacuum expectation values (VEVs) ranging from 1 TeV up to (at least)  $10^3$  TeV – a construction which is presumably responsible for the peculiar quark masses and mixing in the SM. However, the aforementioned neutrino mass problem is set aside noting that, in principle, one could fine tune the contributions of the two Higgs fields, both of which are  $\mathcal{O}(v_{EW})$  where  $v_{EW} \approx 246$  GeV.

Also relevant to this article is the idea of Ref. [32], where the authors consider an extended color symmetry  $SU(3)_{12} \times SU(3)_3 \rightarrow SU(3)_c$ , where the first two quark families are charged under  $SU(3)_{12}$ , and the third family is charged under  $SU(3)_3$ . An approximate  $U(2)$  flavor symmetry [33] is obtained accidentally as an artifact of the gauge representation choices. The leading  $U(2)$  breaking spurion is gen-

\* admgrelj@uni-mainz.de

† bstefan@uni-mainz.de

<sup>1</sup> As shown in [16], the “4321” model is the first UV complete gauge model to coherently address a set of experimental anomalies recently reported in semi-leptonic  $B$ -meson decays [19–25], utilizing the vector LQ representation  $U_1^\mu = (\mathbf{3}, \mathbf{1}, 2/3)$ . See also recent activities in Refs. [26–31].



Submitted to: Phys. Rev. Lett.

CERN-EP-2017-334  
February 14, 2018

arXiv:1802.04329v1 [hep-ex] 12 Feb 2018

# Search for the Decay of the Higgs Boson to Charm Quarks with the ATLAS Experiment

The ATLAS Collaboration

A direct search for the Standard Model Higgs boson decaying to a pair of charm quarks is presented. Associated production of the Higgs and Z bosons, in the decay mode  $ZH \rightarrow \ell^+ \ell^- c\bar{c}$  is studied. A dataset with an integrated luminosity of  $36.1 \text{ fb}^{-1}$  of  $pp$  collisions at  $\sqrt{s} = 13 \text{ TeV}$  recorded by the ATLAS experiment at the LHC is used. The  $H \rightarrow c\bar{c}$  signature is identified using charm-tagging algorithms. The observed (expected) upper limit on  $\sigma(pp \rightarrow ZH) \times \mathcal{B}(H \rightarrow c\bar{c})$  is  $2.7 (3.9^{+2.1}_{-1.1}) \text{ pb}$  at the 95% confidence level for a Higgs boson mass of 125 GeV, while the Standard Model value is 26 fb.

© 2018 CERN for the benefit of the ATLAS Collaboration.  
Reproduction of this article or parts of it is allowed as specified in the CC-BY-4.0 license.

Herakleitos, Thales and Aristeia programmes co-financed by EU-ESF and the Greek NSRF; BSF, GIF and Minerva, Israel; BRF, Norway; CERCA Programme Generalitat de Catalunya, Generalitat Valenciana, Spain; the Royal Society and Leverhulme Trust, United Kingdom.

The crucial computing support from all WLCG partners is acknowledged gratefully, in particular from CERN, the ATLAS Tier-1 facilities at TRIUMF (Canada), NDGF (Denmark, Norway, Sweden), CC-IN2P3 (France), KIT/GridKA (Germany), INFN-CNAF (Italy), NL-T1 (Netherlands), PIC (Spain), ASGC (Taiwan), RAL (UK) and BNL (USA), the Tier-2 facilities worldwide and large non-WLCG resource providers. Major contributors of computing resources are listed in Ref. [70].

## References

- [1] ATLAS Collaboration, *Observation of a new particle in the search for the Standard Model Higgs boson with the ATLAS detector at the LHC*, *Phys. Lett. B* **716** (2012) 1, arXiv: [1207.7214 \[hep-ex\]](#).
- [2] CMS Collaboration, *Observation of a new boson with mass near 125 GeV in pp collisions at  $\sqrt{s} = 7$  and 8 TeV*, *JHEP* **06** (2013) 081, arXiv: [1303.4571 \[hep-ex\]](#).
- [3] L. Evans and P. Bryant, *LHC Machine*, *JINST* **3** (2008) S08001.
- [4] ATLAS Collaboration, *Measurements of the Higgs boson production and decay rates and coupling strengths using pp collision data at  $\sqrt{s} = 7$  and 8 TeV in the ATLAS experiment*, *Eur. Phys. J. C* **76** (2016) 6, arXiv: [1507.04548 \[hep-ex\]](#).
- [5] CMS Collaboration, *Precise determination of the mass of the Higgs boson and tests of compatibility of its couplings with the standard model predictions using proton collisions at 7 and 8 TeV*, *Eur. Phys. J. C* **75** (2015) 212, arXiv: [1412.8662 \[hep-ex\]](#).
- [6] CMS Collaboration, *Study of the Mass and Spin-Parity of the Higgs Boson Candidate Via Its Decays to Z Boson Pairs*, *Phys. Rev. Lett.* **110** (2013) 081803, arXiv: [1212.6639 \[hep-ex\]](#).
- [7] ATLAS Collaboration, *Evidence for the spin-0 nature of the Higgs boson using ATLAS data*, *Phys. Lett. B* **726** (2013) 120, arXiv: [1307.1432 \[hep-ex\]](#).
- [8] CMS Collaboration, *Constraints on the spin-parity and anomalous HVV couplings of the Higgs boson in proton collisions at 7 and 8 TeV*, *Phys. Rev. D* **92** (2015) 012004, arXiv: [1411.3441 \[hep-ex\]](#).
- [9] ATLAS and CMS Collaborations, *Measurements of the Higgs boson production and decay rates and constraints on its couplings from a combined ATLAS and CMS analysis of the LHC pp collision data at  $\sqrt{s} = 7$  and 8 TeV*, *JHEP* **08** (2016) 045, arXiv: [1606.02266 \[hep-ex\]](#).
- [10] ATLAS and CMS Collaborations, *Combined Measurement of the Higgs Boson Mass in pp Collisions at  $\sqrt{s} = 7$  and 8 TeV with the ATLAS and CMS Experiments*, *Phys. Rev. Lett.* **114** (2015) 191803, arXiv: [1503.07589 \[hep-ex\]](#).
- [11] ATLAS Collaboration, *Evidence for the associated production of the Higgs boson and a top quark pair with the ATLAS detector*, (2017), arXiv: [1712.08891 \[hep-ex\]](#).

# Perfect fluid Lagrangian and its cosmological implications in theories of gravity with non-minimally coupled matter fields

P.P. Avelino\*

*Instituto de Astrofísica e Ciências do Espaço, Universidade do Porto,  
CAUP, Rua das Estrelas, PT4150-762 Porto, Portugal  
Centro de Astrofísica da Universidade do Porto,  
Rua das Estrelas, PT4150-762 Porto, Portugal and  
Departamento de Física e Astronomia, Faculdade de Ciências,  
Universidade do Porto, Rua do Campo Alegre 687, PT4169-007 Porto, Portugal*

R.P.L. Azevedo†

*Centro de Física do Porto and  
Departamento de Física e Astronomia, Faculdade de Ciências,  
Universidade do Porto, Rua do Campo Alegre 687, PT4169-007 Porto, Portugal  
(Dated: February 14, 2018)*

In this paper we show that the on-shell Lagrangian of a perfect fluid depends on microscopic properties of the fluid, giving specific examples of perfect fluids with different on-shell Lagrangians but with the same energy-momentum tensor. We demonstrate that if the fluid is constituted by localized concentrations of energy with fixed rest mass and structure (solitons) then the average on-shell Lagrangian of a perfect fluid is given by  $\mathcal{L}_m = T$ , where  $T$  is the trace of the energy-momentum tensor. We show that our results have profound implications for theories of gravity where the matter Lagrangian appears explicitly in the equations of motion of the gravitational and matter fields, potentially leading to observable deviations from a nearly perfect cosmic microwave background black body spectrum:  $n$ -type spectral distortions, affecting the normalization of the spectral energy density. Finally, we put stringent constraints on  $f(R, \mathcal{L}_m)$  theories of gravity using the COBE-FIRAS measurement of the spectral radiance of the cosmic microwave background.

## I. INTRODUCTION

In some theories of gravity the matter Lagrangian enters explicitly in the equations of motion of the gravitational and matter fields, thus making the quest for the appropriate form of the Lagrangian a relevant one, in particular in the case where the energy-momentum tensor of the matter fields is described by a perfect fluid. In [1], by choosing a specific form of the action for a perfect fluid, it has been shown that, in the context of General Relativity (GR), the on-shell Lagrangian of a perfect fluid is equal to  $\mathcal{L}_m = p$ , where  $p$  is the proper pressure. There it has also been noted that the addition of appropriate surface integrals to the action would lead to  $\mathcal{L}_m = -\rho$ , where  $\rho$  is the proper energy density, without affecting the equations of motion. Although this degeneracy has no observable consequences in the context of GR, in theories of gravity where the matter Lagrangian appears explicitly in the equations of motion of the gravitational and matter fields, such as  $f(R, \mathcal{L}_m)$  [2, 3] and  $f(R, T)$  [4] theories of gravity, the dynamics of the gravitational and matter fields may be significantly different depending on whether one considers  $\mathcal{L}_m = p$  or  $\mathcal{L}_m = -\rho$  as the Lagrangian of a perfect fluid [5]. Nevertheless, in [6] it has been argued that  $\mathcal{L}_m = -\rho$  is the correct choice for non-

minimally coupled (NMC) theories, a suggestion that has been followed in some of the subsequent works investigating astrophysical and cosmological consequences of such theories (see, e.g. [7–10]).

In [11] (see also [12]) the Lagrangian of a barotropic perfect fluid whose proper pressure is a function solely of the rest mass density was derived from the equations of motion, with minimal assumptions about the gravitational theory — it was assumed that the matter Lagrangian is independent of the derivatives of the metric and that the particle number is conserved. Still, even in the simplest cases relevant to cosmology, the proper pressure depends not only on the rest mass density (i.e. the proper number density times the rest mass of the particles), but also on the root mean square velocity of the particles. Moreover, the assumed dependence of the Lagrangian on the rest mass density, rather than the energy density, limits the application of the result presented in [12] to the observed content of our Universe, even during the radiation era.

In the present paper we revisit the problem of finding the on-shell Lagrangian of a perfect fluid, focusing on its dependence on the microscopic properties of the fluid. We start, in Sec. II, by briefly reviewing the equations of motion of the gravitational and matter fields in the context of  $f(R, \mathcal{L}_m)$  gravity. In Sec. III we explicitly demonstrate that the on-shell Lagrangian of a perfect fluid depends on the microscopic properties of the fluid not specified by its energy-momentum tensor. By modelling particles as topological solitons in 1+1 dimensions,

\*Electronic address: pedro.avelino@astro.up.pt

†Electronic address: rplazevedo@fc.up.pt

# Impacts of gravitational-wave standard siren observation of the Einstein Telescope on weighing neutrinos in cosmology

Ling-Feng Wang,<sup>1</sup> Xuan-Neng Zhang,<sup>1</sup> Jing-Fei Zhang,<sup>1</sup> and Xin Zhang<sup>\*1, 2, †</sup>

<sup>1</sup>*Department of Physics, College of Sciences, Northeastern University, Shenyang 110004, China*

<sup>2</sup>*Center for High Energy Physics, Peking University, Beijing 100080, China*

We investigate the impacts of the gravitational-wave (GW) standard siren observation of the Einstein Telescope (ET) on constraining the total neutrino mass. We simulate 1000 GW events observed by the ET in the future 10 years by taking the standard  $\Lambda$ CDM cosmology as a fiducial model. We combine the simulated GW data with other cosmological observations including cosmic microwave background (CMB), baryon acoustic oscillations (BAO), and type Ia supernovae (SN). We consider three mass hierarchy cases for the neutrino mass, i.e., normal hierarchy (NH), inverted hierarchy (IH), and degenerate hierarchy (DH). Using Planck+BAO+SN, we obtain  $\sum m_\nu < 0.175$  eV for the NH case,  $\sum m_\nu < 0.200$  eV for the IH case, and  $\sum m_\nu < 0.136$  eV for the DH case. After considering the GW data, i.e., using Planck+BAO+SN+GW, the constraint results become  $\sum m_\nu < 0.151$  eV for the NH case,  $\sum m_\nu < 0.185$  eV for the IH case, and  $\sum m_\nu < 0.122$  eV for the DH case. We find that the GW data can help reduce the upper limits of  $\sum m_\nu$  by 13.7%, 7.5%, and 10.3% for the NH, IH, and DH cases, respectively. Besides, we find that the GW data can also help break the degeneracies between  $\sum m_\nu$  and other parameters. We show that the GW data of the ET could greatly improve the constraint accuracies of cosmological parameters.

## I. INTRODUCTION

On 17 August 2017, the signal of gravitational wave (GW) produced by the merger of a binary neutron-star system (BNS) was detected for the first time [1], and the electromagnetic (EM) signals generated by the same transient source were also observed subsequently, which indicates that the age of gravitational-wave multimessenger astronomy is coming. The measurement of GWs from the merger of a binary compact-object system involves the information of absolute luminosity distance of the transient source [2], and thus if we can simultaneously accurately measure the GW and EM signals from the same merger event of a BNS or a binary system consisting of a neutron star (NS) and a black hole (BH), then we are able to establish a true luminosity distance–redshift ( $d_L$ – $z$ ) relation. Therefore, the GW observations can serve as a cosmic “standard siren”, which can be developed to be a new cosmological probe if we can accurately observe a large number of merger events of this class.

The current mainstream cosmological probes include the measurements of cosmic microwave background (CMB) anisotropies (temperature and polarization), baryon acoustic oscillations (BAO), type Ia supernovae (SNIa), and the Hubble constant, etc. In addition, there are also some observations for the growth history of large-scale structure (LSS), such as the shear measurement of the weak gravitational lensing, the galaxy clusters number counts in light of Sunyaev-Zeldovich (SZ) effect, and the CMB lensing measurement, etc. When using these observational data to make cosmological parameter esti-

mation, some problems occur including mainly: (i) there are degeneracies between some parameters, and in some of which the correlations are rather strong, and (ii) there are apparent tensions between some observations. The GW standard siren observations have some peculiar advantages in breaking the parameter degeneracies, owing to the fact that the GW observations can directly measure the true luminosity distances, but the SNIa observations actually can only measure the differences of luminosity distances at different redshifts, but not the true luminosity distances. In addition, compared to the standard candle provided by the SNIa observations [3–5], which needs to cross-calibrate the distance indicators on different scales, the GW observations allows us to directly measure the luminosity distances up to higher redshifts [6]. To obtain the information of redshifts, one needs to find the EM counterparts of the GW sources. In fact, there are some forthcoming large facility observation programs, such as Large Synoptic Survey Telescope (LSST) [7], Square Kilometer Array (SKA) [8], and Extremely Large Telescope (ELT) [9], which can detect the EM counterparts by optically identifying the host galaxies. In this way, in the near future, the  $d_L$ – $z$  relation would be obtained by the GW standard siren measurements, and we could use this powerful tool to explore the expansion history of the universe.

Recently, the related issues have been discussed by some authors [10–17] (see also Ref. [18] for a recent review). For example, in Ref. [10], Cai and Yang estimated the ability of using GW data to constrain cosmological parameters. They considered to use the GW detector in construction, the Einstein Telescope (ET), to simulate the GW data, which is a third-generation ground-based detector of GWs [19]. ET is ten times more sensitive than the current advanced ground-based detectors and it covers the frequency range of  $1 - 10^4$  Hz. According to their results [10], the errors of cosmological parameters can be

\*Corresponding author

†Electronic address: zhangxin@mail.neu.edu.cn

# Cosmological bounds on neutrino statistics

P.F. de Salas,<sup>a</sup> S. Gariazzo,<sup>a</sup> M. Laveder,<sup>b</sup> S. Pastor,<sup>a</sup> O. Pisanti<sup>c</sup>  
and N. Truong<sup>d,e</sup>

<sup>a</sup>Instituto de Física Corpuscular (CSIC-Universitat de València)  
Parc Científic UV, C/ Catedrático José Beltrán, 2  
E-46980 Paterna (Valencia), Spain

<sup>b</sup>Dipartimento di Fisica e Astronomia “G. Galilei”, Università di Padova,  
and INFN, Sezione di Padova, Via F. Marzolo 8, I-35131 Padova, Italy

<sup>c</sup>Dipartimento di Fisica E. Pancini, Università di Napoli Federico II,  
and INFN, Sezione di Napoli, Via Cintia, I-80126 Napoli, Italy.

<sup>d</sup>MTA-Eötvös University Lendület Hot Universe Research Group  
Pázmány Péter sétány 1/A, Budapest, 1117, Hungary

<sup>e</sup>Institute For Interdisciplinary Research in Science and Education  
ICISE, Ghenh Rang, 590000 Quy Nhon, Vietnam

E-mail: [pabferde@ific.uv.es](mailto:pabferde@ific.uv.es), [gariazzo@ific.uv.es](mailto:gariazzo@ific.uv.es), [marco.laveder@pd.infn.it](mailto:marco.laveder@pd.infn.it),  
[pastor@ific.uv.es](mailto:pastor@ific.uv.es), [pisanti@na.infn.it](mailto:pisanti@na.infn.it), [truongnhut@caesar.elte.hu](mailto:truongnhut@caesar.elte.hu)

**Abstract.** We consider the phenomenological implications of the violation of the Pauli exclusion principle for neutrinos, focusing on cosmological observables such as the spectrum of Cosmic Microwave Background anisotropies, Baryon Acoustic Oscillations and the primordial abundances of light elements. Neutrinos that behave (at least partly) as bosonic particles have a modified equilibrium distribution function that implies a different influence on the evolution of the Universe that, in the case of massive neutrinos, can not be simply parametrized by a change in the effective number of neutrinos. Our results show that, despite the precision of the available cosmological data, only very weak bounds can be obtained on neutrino statistics, disfavouring a more *bosonic* behaviour at less than  $2\sigma$ .

# Pseudorapidity distribution and decorrelation of anisotropic flow within CLVisc hydrodynamics

Long-Gang Pang<sup>1,2,3,4</sup>, Hannah Petersen<sup>4,5,6</sup>, Xin-Nian Wang<sup>1,2,3</sup>

<sup>1</sup>*Key Laboratory of Quark & Lepton Physics (MOE) and Institute of Particle Physics, Central China Normal University, Wuhan 430079, China*

<sup>2</sup>*Physics Department, University of California, Berkeley, CA 94720, USA*

<sup>3</sup>*Nuclear Science Division, Lawrence Berkeley National Laboratory, Berkeley, CA 94720, USA*

<sup>4</sup>*Frankfurt Institute for Advanced Studies, Ruth-Moufang-Strasse 1, 60438 Frankfurt am Main, Germany*

<sup>5</sup>*Institute for Theoretical Physics, Goethe University,*

*Max-von-Laue-Strasse 1, 60438 Frankfurt am Main, Germany and*

<sup>6</sup>*GSI Helmholtzzentrum für Schwerionenforschung, Planckstr. 1, 64291 Darmstadt, Germany*

Studies of fluctuations and correlations of soft hadrons and hard and electromagnetic probes of the dense and strongly interacting medium require event-by-event hydrodynamic simulations of high-energy heavy-ion collisions that are computing intensive. We develop a (3+1)D viscous hydrodynamic model – CLVisc that is parallelized on Graphics Processing Unit (GPU) using Open Computing Language (OpenCL) with 60 times performance increase for space-time evolution and more than 120 times for the Cooper-Frye particlization relative to that without GPU parallelization. The model is validated with comparisons with different analytic solutions, other existing numerical solutions of hydrodynamics and experimental data on hadron spectra in high-energy heavy-ion collisions. The pseudo-rapidity dependence of anisotropic flow  $v_n(\eta)$  are then computed in CLVisc with initial conditions given by the A Multi-Phase Transport (AMPT) model, with energy density fluctuations both in the transverse plane and along the longitudinal direction. Although the magnitude of  $v_n(\eta)$  and the ratios between  $v_2(\eta)$  and  $v_3(\eta)$  are sensitive to the effective shear viscosity over entropy density ratio  $\eta_v/s$ , the shape of the  $v_n(\eta)$  distributions in  $\eta$  do not depend on the value of  $\eta_v/s$ . The decorrelation of  $v_n$  along the pseudo-rapidity direction due to the twist and fluctuation of the event-planes in the initial parton density distributions is also studied. The decorrelation observable  $r_n(\eta^a, \eta^b)$  between  $v_n\{-\eta^a\}$  and  $v_n\{\eta^a\}$  with the auxiliary reference window  $\eta^b$  is found not sensitive to  $\eta_v/s$  when there is no initial fluid velocity. For small  $\eta_v/s$ , the initial fluid velocity from mini-jet partons introduces sizable splitting of  $r_n(\eta^a, \eta^b)$  between the two reference rapidity windows  $\eta^b \in [3, 4]$  and  $\eta^b \in [4.4, 5.0]$ , as has been observed in experiment. The implementation of CLVisc and guidelines on how to efficiently parallelize scientific programs on GPUs are also provided.

PACS numbers: 12.38.Mh, 25.75.Ld, 25.75.Gz

## I. INTRODUCTION

Heavy-ion collisions at the Relativistic Heavy-Ion Collider (RHIC) and Large Hadron Collider (LHC) create strongly coupled QCD matter that exhibits multiple extreme properties. It is the hottest – temperature reaching more than 100,000 times that at the core of the Sun, most vortical – angular momentum on the order of  $10^3 - 10^5 \hbar$  [1] and almost perfect fluid – very low shear viscosity over entropy density ratio [2–4], that is exposed to the strongest magnetic field ( $|\mathbf{B}| = 5 \sim 10 m_\pi^2$ ) [5] ever produced in laboratory. This strongly coupled QCD matter is believed to share some of the properties of the quark-gluon-plasma epoch in the early universe.

Numerical simulations of the dynamical evolution of this strongly coupled QCD matter and comparisons with experimental data are vital to extract the physical properties of the strong interaction matter. Relativistic viscous hydrodynamics is the most successful effective theory in describing the space-time evolution of QCD matter created in high-energy heavy-ion collisions [6, 7]. Hybrid approaches that comprise hydrodynamics and hadronic transport agree with experimental data on various observables such as charged multiplicity, transverse momen-

tum spectra and transverse momentum  $p_T$ -differential elliptic flow of identical particles [8] (and references therein). Event-by-event simulations with energy density fluctuations [9–18] in the initial states are indispensable to describe not only the ensemble average of odd-order harmonic flows but also their probability distributions [19]. New observables such as the correlation between different event plane angles [20–23], different harmonic flows [24] and  $p_T$ -differential harmonic flows [25] can provide more rigorous constraints on medium properties such as the shear viscosity to entropy density ratio, but also require efficient algorithms to reach sufficient statistics in a reasonable amount of CPU time. Furthermore, (3+1)D event-by-event hydrodynamics is also necessary to understand the longitudinal structure of the collective flow. The initial state fluctuations along the longitudinal direction have been built in many models [26–33]. Observables [34–43] have been designed to either constrain the longitudinal structure in the initial state or to determine other QGP properties using the multiplicity or anisotropic flow correlations along the longitudinal direction. Taking into account the asymmetry between forward and backward going participants, the non-central heavy-ion collisions not only produce strong angular mo-

# Strangeness $S = -1$ hyperon-nucleon interactions: chiral effective field theory vs. lattice QCD

Jing Song,<sup>1</sup> Kai-Wen Li,<sup>1,2</sup> and Li-Sheng Geng<sup>1,3,4,\*</sup>

<sup>1</sup>*School of Physics and Nuclear Energy Engineering and International  
Research Center for Nuclei and Particles in the Cosmos,*

*Beihang University, Beijing 100191, China*

<sup>2</sup>*Yukawa Institute for Theoretical Physics,  
Kyoto University, Kyoto 606-8502, Japan*

<sup>3</sup>*Beijing Key Laboratory of Advanced Nuclear Materials and Physics,  
Beihang University, Beijing 100191, China*

<sup>4</sup>*Beijing Advanced Innovation Center for Big Data-based Precision Medicine,  
Beihang University, Beijing, 100191, China*

(■Dated: February 14, 2018)

## Abstract

Hyperon-nucleon interactions serve as basic inputs to studies of hypernuclear physics and dense (neutron) stars. Unfortunately, a precise understanding of these important quantities have lagged far behind that of the nucleon-nucleon interaction due to lack of high precision experimental data. Historically, hyperon-nucleon interactions are either formulated in quark models or meson exchange models. In recent years, lattice QCD simulations and chiral effective field theory approaches start to offer new insights from first principles. In the present work, we contrast the state of art lattice QCD simulations with the latest chiral hyperon-nucleon forces and show that the leading order relativistic chiral results can already describe the lattice QCD data reasonably well. Given the fact that the lattice QCD simulations are performed with pion masses ranging from the (almost) physical point to 700 MeV, such studies provide a highly non-trivial check on both the chiral effective field theory approaches as well as lattice QCD simulations. Nevertheless more precise lattice QCD simulations are eagerly needed to refine our understanding of hyperon-nucleon interactions.

---

\* E-mail me at: lisheng.geng@buaa.edu.cn



# Constraints on Einstein-aether theory after GW170817

Jacob Oost<sup>a,\*</sup>, Shinji Mukohyama<sup>b,c,†</sup> and Anzhong Wang<sup>a,d,‡</sup>

<sup>a</sup> GCAP-CASPER, Physics Department, Baylor University, Waco, TX 76798-7316, USA

<sup>b</sup> Center for Gravitational Physics, Yukawa Institute for Theoretical Physics, Kyoto University, 606-8502, Kyoto, Japan

<sup>c</sup> Kavli Institute for the Physics and Mathematics of the Universe (WPI),

The University of Tokyo Institutes for Advanced Study,

The University of Tokyo, Kashiwa, Chiba 277-8583, Japan

<sup>d</sup> Institute for Advanced Physics & Mathematics,

Zhejiang University of Technology, Hangzhou 310032, China

(Dated: February 14, 2018)

In this paper, we carry out a systematic analysis of the theoretical and observational constraints on the dimensionless coupling constants  $c_i$  ( $i = 1, 2, 3, 4$ ) of the Einstein-aether theory, taking into account the events GW170817 and GRB 170817A. The combination of these events restricts the deviation of the speed of the spin-2 graviton  $c_T$  to the range,  $-3 \times 10^{-15} < c_T - 1 < 7 \times 10^{-16}$ , which for the Einstein-aether theory implies  $|c_{13}| \leq 10^{-15}$  with  $c_{13} \equiv c_1 + c_3$ . The rest of the constraints are divided into two groups: those on the  $(c_1, c_{14})$ -plane and those on the  $(c_2, c_{14})$ -plane, where  $c_{14} \equiv c_1 + c_4$ , except for the strong-field constraints. The strong-field constraints depend on the sensitivities  $\sigma_{\text{ns}}$  of neutron stars, which are not known at present in the new ranges of the parameters found in this paper.

## I. INTRODUCTION

The invariance under the Lorentz symmetry group is a cornerstone of modern physics and strongly supported by experiments and observations [1]. Nevertheless, there are various reasons to construct gravitational theories with broken Lorentz invariance (LI) [2]. For example, if space and/or time at the Planck scale are/is discrete, as currently it is understood [3], Lorentz symmetry is absent at short distance/time scales and must be an emergent low energy symmetry. A concrete example of gravitational theories with broken LI is the Hořava theory of quantum gravity [4], in which the LI is broken via the anisotropic scaling between time and space in the ultraviolet (UV),  $t \rightarrow b^{-z}t$ ,  $x^i \rightarrow b^{-1}x^i$ , ( $i = 1, 2, \dots, d$ ), where  $z$  denotes the dynamical critical exponent, and  $d$  the spatial dimensions. Power-counting renormalizability requires  $z \geq d$  at short distances, while LI demands  $z = 1$ . For more details about Hořava gravity, see, for example, the recent review [5].

Another theory that breaks LI is the Einstein-aether theory [6], in which LI is broken by the existence of a preferred frame defined by a time-like unit vector field, the so-called aether field. The Einstein-aether theory is a low energy effective theory and passes all theoretical and observational constraints by properly choosing the coupling constants of the theory [7], including the stability of the Minkowski spacetime [8], the abundance of the light elements formed in the early universe [9], gravi-Cerenkov effects [10], the Solar System observations [11], binary pulsars [12, 13], and more recently gravitational

waves [14].

Among the 10 parameterized post-Newtonian (PPN) parameters [15] in the Einstein-aether theory, the only two parameters that deviate from general relativity are  $\alpha_1$  and  $\alpha_2$ , which measure the preferred frame effects. In terms of the four dimensionless coupling constants  $c_i$ 's of the Einstein-aether theory, they are given by [11],

$$\begin{aligned}\alpha_1 &= -\frac{8(c_3^2 + c_1c_4)}{2c_1 - c_1^2 + c_3^2}, \\ \alpha_2 &= \frac{1}{2}\alpha_1 - \frac{(c_1 + 2c_3 - c_4)(2c_1 + 3c_2 + c_3 + c_4)}{c_{123}(2 - c_{14})},\end{aligned}\quad (1.1)$$

where  $c_{ij} \equiv c_i + c_j$  and  $c_{ijk} \equiv c_i + c_j + c_k$ . In the weak-field regime, using lunar laser ranging and solar alignment with the ecliptic, Solar System observations constrain these parameters to very small values [15],

$$|\alpha_1| \leq 10^{-4}, \quad |\alpha_2| \leq 10^{-7}. \quad (1.2)$$

Considering the smallness of  $\alpha_A$  ( $A = 1, 2$ ), it may be convenient to Taylor expand Eq.(1.1) with respect to  $\alpha_A$  to obtain

$$c_2 = -\frac{c_{13}(2c_1 - c_3)}{3c_1} + \mathcal{O}(\alpha_A), \quad c_4 = -\frac{c_3^2}{c_1} + \mathcal{O}(\alpha_A). \quad (1.3)$$

If terms of order  $\mathcal{O}(\alpha_A)$  and higher are small enough to be neglected then the four-dimensional parameter space spanned by  $c_i$ 's reduces to two-dimensional one. Until recently, the strongest constraints on the Einstein-aether theory were (1.2) and thus this treatment was a good approximation. Then, using the order-of-magnitude arguments about the orbital decay of binary pulsars, Foster estimated that  $|c_1 \pm c_3| \lesssim \mathcal{O}(10^{-2})$ , by further assuming that  $c_i \ll 1$  [12]. More detailed analysis of binary pulsars showed that  $c_{13} \lesssim \mathcal{O}(10^{-2})$ ,  $|c_1 - c_3| \lesssim \mathcal{O}(10^{-3})$ , see Fig. 1 in [13].

<sup>‡</sup>The corresponding author

<sup>\*</sup>Electronic address: Jacob.Oost@baylor.edu

<sup>†</sup>Electronic address: shinji.mukohyama@yukawa.kyoto-u.ac.jp

<sup>‡</sup>Electronic address: anzhong.wang@baylor.edu

# Distinguishing rotating Kiselev black hole from naked singularity using spin precession of test gyroscope

Muhammad Rizwan,<sup>1,\*</sup> Mubasher Jamil,<sup>1,†</sup> and Anzhong Wang<sup>‡2,§</sup>

<sup>1</sup>*Department of Mathematics, School of Natural Sciences (SNS),  
National University of Sciences and Technology (NUST), H-12, Islamabad, Pakistan*

<sup>2</sup>*GCAP-CASPER, Physics Department, Baylor University, Waco, TX 76798-7316, USA*

*Institute for Advanced Physics & Mathematics, Zhejiang University of Technology, Hangzhou, 310032, China*

We study the critical values  $(\alpha_c, a_c)$  of the quintessential and spin parameters, to distinguish a rotating Kiselev black hole (RKBH) from a naked singularity. For any value of the dimensionless quintessential parameter  $\omega_q \in (-1, -1/3)$ , a black hole can exist if  $\alpha \leq \alpha_c$  and  $a \leq a_c$ . Both  $\alpha_c$  and  $a_c$  are directly proportional to  $\omega_q$ . Further, for any  $\omega_q$ , when increasing the value of  $\alpha$  from zero to  $\alpha_c$ , the size of the event horizon increases, whereas the size of the outer horizon decreases. We also study the critical value of the quintessential parameter  $\bar{\alpha}_c$  for the Kiselev black hole (KBH) and find horizons of extremal black holes. It is seen that, similar to a RKBH, for a KBH with any  $\omega_q$ , when increasing the value of  $\alpha$ , the size of the event horizon increases, while the size of the outer horizon decreases. We then study the spin precession of a test gyroscope attached to a stationary observer in this spacetime. Using the spin precessions we differentiate black holes from naked singularities. If the precession frequency becomes arbitrarily large, as approaching to the central object in the quintessential field along any direction, then the spacetime is a black hole. A spacetime will contain a naked singularity if the precession frequency remains finite everywhere except at the singularity itself. Finally, we study the Lense-Thirring precession frequency for RKBHs and the geodetic precession for KBHs.

**Keywords:** Black hole; Geodetic precession; Quintessential matter; Singularity; Spin precession.

## I. INTRODUCTION

Current research on observational measurements predicts the accelerating expansion of Universe, which is due to a valuable presence of state with the negative pressure [1, 2]. The negative pressure could be due to a cosmological constant or a so-called “quintessence matter” with an equation of state  $p = \omega_q \rho$ , where the dimensionless quintessential parameter  $\omega_q$  is  $-1 < \omega_q < -1/3$ ,  $p$  and  $\rho$  represent, respectively, the pressure  $p$  and energy density  $\rho$  of the quintessence field. If the quintessence matter exists all over the Universe, it can also be around a black hole. The spherically symmetric static black hole in a quintessential matter field is known as the Kiselev black hole [2]. Thermodynamics and phase transition of the charged KBH were studied in [3–5]. The strong gravitational lensing by a KBH and a charged KBH has been discussed in [7, 8]. Recently, using Newman and Janis’ technique [9] and its modification [10], rotational generalization of a KBH have been given in [11]. The Kerr-Newman-AdS black hole solution in a quintessential matter field has been also obtained in [12].

Due to the rotation of the central object, spacetime exhibits effects of the Lense-Thirring (LT) precession, which causes the dragging of locally inertial frames along the rotating spacetime [13–15]. Due to these effects a gyroscope attached to stationary observers in such a spacetime precesses with certain frequencies. In the weak field approximations the magnitude of the precession frequency is proportional to the spin parameter of the central object and decreases with a cubic order of the distance from the central object [14, 15]. The gyroscope also precesses due to the spacetime curvature of the central object and this type of precessions is known as geodesic precessions or de Sitter precessions [16, 17]. The LT-precession in the strong gravitational field of the Kerr and Kerr-Taub-NUT black holes has been discussed in [18]. The geodetic precession in the KBH has been studied in [6]. To measure the precession rate due to the LT and geodetic effects relative to the Copernican system or the fixed star HR8703, known as IM Pegasi, of a test gyro due to the rotation of the Earth has been launched [19].

During the gravitational collapse of massive stars, the existence of naked singularities is the topic of great interest for researchers in the field of gravitational theory and relativistic astrophysics. The key question is that how one can differentiate whether the ultimate product in the life cycle of the compact object under the self-gravity collapse is

<sup>‡</sup> The corresponding author

<sup>\*</sup>Electronic address: m.rizwan@sns.nust.edu.pk

<sup>†</sup>Electronic address: m.jamil@sns.nust.edu.pk

<sup>§</sup>Electronic address: anzhong\_wang@baylor.edu

# Study of temporal quantum correlations in decohering $B$ and $K$ meson systems

Javid Naikoo,<sup>\*</sup> Ashutosh Kumar Alok,<sup>†</sup> and Subhashish Banerjee<sup>‡</sup>

*Indian Institute of Technology Jodhpur, Jodhpur 342011, India*

(Dated: February 14, 2018)

In this work we study temporal quantum correlations, quantified by Leggett-Garg (LG) and LG-type inequalities, in the  $B$  and  $K$  meson systems. We use the tools of open quantum systems to incorporate the effect of decoherence which is quantified by a single phenomenological parameter. The effect of  $CP$  violation is also included in our analysis. We find that the LG inequality is violated for both  $B$  and  $K$  meson systems, the violation being most prominent in the case of  $K$  mesons and least for  $B_s$  system. Since the systems with no coherence do not violate LGI, incorporating *decoherence* is expected to decrease the extent of violation of LGI and is clearly brought out in our results. We show that the expression for the LG functions depends upon an additional term, apart from the experimentally measurable meson transition probabilities. This term vanishes in the limit of zero decoherence. On the other hand, the LG-type parameter can be directly expressed in terms of transition probabilities, making it a more appropriate observable for studying temporal quantum correlations in neutral meson systems.

## I. INTRODUCTION

Quantum correlations (QCs), existing between two or more parties [1, 2], are bestowed with properties unique to the quantum world and are of pivotal importance in quantum information science. The study of QCs not only unveils the fundamental traits responsible for the distinction of the quantum mechanically correlated systems from those attributed with a joint classical probability distribution [3], it also helps in devising efficient ways of carrying out the tasks of quantum communication and computation [4–6].

Among the most celebrated notions in quantum physics are nonlocality [7], entanglement [1], quantum discord [8, 9], and teleportation fidelity [10, 11]. These spatial quantum correlations (SQC) have enhanced our understanding of nature at the fundamental level and at the same time have provided efficacious solutions in the development of the theory of quantum information. The SQCs mentioned above have been studied in many systems, viz., optical systems [12–18], NMR [19–21], neutrino oscillation [22–25],  $B$  and  $K$  meson systems [26]. Of the above listed SQCs, Bell nonlocality is the strongest and Bell inequalities are considered to be the oldest tool for detecting entanglement [27].

The temporal quantum correlations (TQCs) arising from the sequential measurements on a system at different times, have also been considered as promising candidates in discerning the quantum behavior from the classical. Leggett and Garg inequalities (LGIs) [28] are among the well known TQCs, violation of which is a witness of quantum *coherence* in the system. LGIs have been a topic of study in various theoretical works [29–35] including, in recent times, neutrino oscillations [25, 36, 37] and studied experimentally in systems like superconducting qubits [38, 39], photons [40–43], and NMR [44–46].

Leggett-Garg inequalities are based on the concept of *macrorealism* (MR) and *noninvasive measurability* (NIM). MR means that the system which has available to it two or more macroscopically distinct states, pertaining to an observable  $\hat{Q}$ , always exists in one of these states irrespective of any measurement performed on it. NIM states that, in principle, we can perform the measurement without disturbing the future dynamics of the system [34]. MR and NIM put limits on certain combinations of the two time correlation functions  $C_{ij} = \langle \hat{Q}(t_i) \hat{Q}(t_j) \rangle$ . Quantum systems, however, violate these limits. The simplest form of LGI is the one involving three measurements performed at  $t_0$ ,  $t_1$  and  $t_2$  ( $t_2 > t_1 > t_0$ )

$$K_3 = C_{01} + C_{12} - C_{02}, \quad (1)$$

such that  $-3 \leq K_3 \leq 1$ . The maximum quantum value of  $K_3$  for a two level system is  $\frac{3}{2}$  [28] and has been found to hold for any system, *irrespective* of the number of levels, as long as the measurements are given by just two projectors  $\Pi^\pm$  [47], a fact revealed in several studies [32, 48–50]. It was shown in [51] that in the limit  $N \rightarrow \infty$ , the LGI can be violated up to its maximum algebraic sum.

<sup>\*</sup>Electronic address: [naikoo.1@iitj.ac.in](mailto:naikoo.1@iitj.ac.in)

<sup>†</sup>Electronic address: [akalok@iitj.ac.in](mailto:akalok@iitj.ac.in)

<sup>‡</sup>Electronic address: [subhashish@iitj.ac.in](mailto:subhashish@iitj.ac.in)

# Resonant production of dark photons in positron beam dump experiments

Enrico Nardi,<sup>1,\*</sup> Cristian D. R. Carvajal,<sup>2</sup> Anish Ghoshal,<sup>1,3</sup> Davide Meloni,<sup>3,4</sup> and Mauro Raggi<sup>5</sup>

<sup>1</sup>*INFN, Laboratori Nazionali di Frascati, C.P. 13, I-00044 Frascati, Italy*

<sup>2</sup>*Universidad de Antioquia, Instituto de Física, Calle 70 No. 52-21, Medellín, Colombia*

<sup>3</sup>*Dipartimento di Matematica e Fisica, Università di Roma Tre, I-00146 Rome, Italy*

<sup>4</sup>*INFN, Sezione di Roma Tre, I-00146 Rome, Italy*

<sup>5</sup>*Dipartimento di Fisica, Università di Roma La Sapienza and INFN, Sezione di Roma, I-00185 Rome, Italy*

(Dated: February 14, 2018)

Positrons beam dump experiments have unique features to search for very narrow resonances coupled superweakly to  $e^+e^-$  pairs. Due to the continue loss of energy from soft photon bremsstrahlung, in the first few radiation lengths of the dump a positron beam can continuously scan for resonant production of new resonances via  $e^+$  annihilation off an atomic  $e^-$  in the target. In the case of a dark photon  $A'$  kinetically mixed with the photon, this production mode is of first order in the electromagnetic coupling  $\alpha$ , and thus parametrically enhanced with respect to the  $O(\alpha^2)$   $e^+e^- \rightarrow \gamma A'$  production mode and to the  $O(\alpha^3)$   $A'$  bremsstrahlung in  $e^-$ -nucleon scattering so far considered. If the lifetime is sufficiently long to allow the  $A'$  to exit the dump,  $A' \rightarrow e^+e^-$  decays could be easily detected and distinguished from backgrounds. We explore the foreseeable sensitivity of the Frascati PADME experiment in searching with this technique for the 17 MeV dark photon invoked to explain the  $^8\text{Be}$  anomaly in nuclear transitions.

## INTRODUCTION

Some unquestionable experimental facts, like dark matter (DM), neutrino masses, and the baryon asymmetry of the Universe, cannot be accounted for within the standard model (SM) of particle physics. Physics beyond the SM (BSM) is thus required, which might correspond to a whole new sector containing new particles as well as new interactions. If such a sector exists, there are two possible reasons why it has not been discovered yet: (i) the mass scale of the new particles, including the mediators of the new forces, is well above the energy scale reached so far in laboratory experiments; (ii) the mass scale is within experimental reach, but the couplings between the new particles and the SM are so feeble that the whole new sector has so far remained hidden.

The first possibility keeps being actively investigated mainly in collider experiments, with the current high energy frontier set by the LHC experiments. However, the so far unsuccessful search for new heavy states has triggered in recent years an increasing interest in the second possibility, with many proposals and many new ideas to hunt for new physics at the intensity frontier (see [1, 2] for recent reviews). In particular, the so called dark-photon

(DP) or  $A'$ -boson, that is a massive gauge boson arising from a new  $U(1)'$  symmetry, can be considered as a natural candidate for a superweakly coupled new state, since its dominant interaction with the SM sector might arise solely from a mixed kinetic term  $(\epsilon/2)F'_{\mu\nu}F^{\mu\nu}$  coupling the  $U(1)'$  and QED field strength tensors, with values of  $\epsilon$  naturally falling in a range well below  $10^{-2}$ .

From the phenomenological point of view, light weakly coupled new particles have been invoked to account for discrepancies between SM predictions and experimental results, as for example the measured value of the muon anomalous magnetic moment [3], the value of the proton charge radius as measured in muonic atoms [4–7], or the anomaly observed in excited  $^8\text{Be}$  nuclear decays by the Atomki collaboration [8–10]. This last anomaly is particularly relevant for the present paper since the new experimental technique that we are going to describe appears remarkably well suited to test, at least in some region of the parameter space, the particle physics explanation involving a new gauge boson with mass  $m_{A'} \sim 17\text{ MeV}$  kinetically mixed with the photon [11].

The anomaly consists in the observation of a bump in the opening angle and invariant mass distributions of electron-positron pairs produced in the decays of an excited  $^8\text{Be}$  nucleus [8], which seems unaccountable by known physics. The anomaly has a high statistical signif-

\* Corresponding author, email: [enrico.nardi@lnf.infn.it](mailto:enrico.nardi@lnf.infn.it)

# A minimally broken residual TBM-Klein symmetry and baryogenesis via leptogenesis

Rome Samanta<sup>a\*</sup>, Mainak Chakraborty<sup>b†</sup>

a) Saha Institute of Nuclear Physics, 1/AF Bidhannagar, Kolkata 700064, India,  
Physics and Astronomy, University of Southampton, Southampton, UK (after March, 2018)

b) Centre of Excellence in Theoretical and Mathematical Sciences

Siksha ‘O’Anusandhan (Deemed to be University)

Khandagiri Square, Bhubaneswar 751030, India

February 14, 2018

## Abstract

We investigate the minimally perturbed neutrino mass matrices which at the leading order give rise to Tri-BiMaximal (TBM) mixing due to a residual  $\mathbb{Z}_2 \times \mathbb{Z}_2^{\mu\tau}$  Klein symmetry in the neutrino mass term of the Lagrangian. Starting from the Lagrangian level of Type-I seesaw which contains  $m_D$  and  $M_R$  as constituent matrices, the  $\mathbb{Z}_2^{\mu\tau}$  is broken in  $M_R$  to be consistent with the nonvanishing value of  $\theta_{13}$ . The unbroken  $\mathbb{Z}_2$  leads to constraint relations between the mixing angles  $\theta_{13}$  and  $\theta_{12}$  along with testable predictions on the Dirac CP phase  $\delta$  and the neutrino less double beta decay parameter  $|(M_\nu)_{11}|$ . A full  $\mathbb{Z}_2 \times \mathbb{Z}_2^{\mu\tau}$  symmetry leads to a degeneracy in the eigenvalues of  $M_R$  matrices. Nevertheless, breaking of  $\mathbb{Z}_2^{\mu\tau}$  which is also necessary to generate nonzero  $\theta_{13}$ , lifts that degeneracy. Unlike the standard  $N_1$ -leptogenesis scenario where only the decays from the lightest right handed (RH) neutrino  $N_1$  are relevant, here the decays from all the quasi-degenerate RH neutrinos contribute to the process of baryogenesis via leptogenesis. Flavor dependent Boltzmann equations are solved for heavy neutrino as well as the light leptonic number densities to compute the final baryon asymmetry  $Y_B$ . Using the observed range for the baryon asymmetry, lower and upper bounds on the RH neutrino masses are obtained thereafter.

## 1 Introduction

The structure of the leptonic mixing matrix  $U_{\text{PMNS}}$  has always been the center of attraction in the flavor model building landscape. Until the experimental discovery of a nonvanishing value of the reactor mixing angle  $\theta_{13}$  [1, 2], it was the paradigm of Tri-BiMaximal (TBM) Ansatz of

---

\*rome.samanta@saha.ac.in

†mainak.chakraborty2@gmail.com

# Numerical estimate of minimal active-sterile neutrino mixing for sterile neutrinos at GeV scale

---

**Igor Krasnov and Timofey Grigorin-Ryabov**

*Department of Particle Physics and Cosmology, Physics Faculty, Moscow State University,  
Vorobjevy Gory 1-2, 119991, Moscow, Russia*

*Institute for Nuclear Research of the Russian Academy of Sciences,  
60th October Anniversary Prospect 7a, 117312, Moscow, Russia*

*E-mail:* [iv.krasnov@physics.msu.ru](mailto:iv.krasnov@physics.msu.ru), [timagr615@gmail.com](mailto:timagr615@gmail.com)

**ABSTRACT:** Seesaw mechanism constrains from below mixing between active and sterile neutrinos for fixed sterile neutrino masses. Signal events associated with sterile neutrino decays inside a detector at fixed target experiment are suppressed by the mixing angle to the power of four. Therefore sensitivity of experiments such as SHiP and DUNE should take into account minimal possible values of the mixing angles. We extend the previous study of this subject [1] to a more general case of non-zero CP-violating phases in the neutrino sector. Namely, we provide numerical estimate of minimal value of mixing angles between active neutrinos and two sterile neutrinos with the third sterile neutrino playing no noticeable role in the mixing. Thus we obtain a sensitivity needed to fully explore the seesaw type I mechanism for sterile neutrinos with masses below 2 GeV, that is relevant for the fixed-target experiments. Remarkably, we observe a strong dependence of this result on the lightest active neutrino mass and the neutrino mass hierarchy, not only on the values of CP-violating phases themselves. All these effects sum up to push the limit of experimental confirmation of sterile-active neutrino mixing by several orders of magnitude below the results of [1] from  $10^{-10} - 10^{-11}$  down to  $10^{-12}$  and even to  $10^{-20}$  in parts of parameter space; nonzero CP-violating phases are responsible for that.

**KEYWORDS:** Neutrino Physics, Beyond Standard Model, CP violation

# The LHC Higgs Boson Discovery: Updated implications for Finite Unified Theories and the SUSY breaking scale

S. Heinemeyer<sup>1,2,3\*</sup>, M. Mondragón<sup>4†</sup>, G. Patellis<sup>5‡</sup>, N. Tracas<sup>5§</sup>  
and G. Zoupanos<sup>5,6¶</sup>

<sup>1</sup>*Instituto de Física Teórica, Universidad Autónoma de Madrid Cantoblanco, 28049 Madrid, Spain*

<sup>2</sup>*Campus of International Excellence UAM+CSIC, Cantoblanco, 28049, Madrid, Spain*

<sup>3</sup>*Instituto de Física de Cantabria (CSIC-UC), E-39005 Santander, Spain*

<sup>4</sup>*Instituto de Física, Universidad Nacional Autónoma de México, A.P. 20-364, México 01000*

<sup>5</sup>*Physics Department, Nat. Technical University, 157 80 Zografou, Athens, Greece*

<sup>6</sup>*Max-Planck Institut für Physik, Föhringer Ring 6, D-80805 München, Germany*

## Abstract

Finite Unified Theories (FUTs) are  $N = 1$  supersymmetric Grand Unified Theories which can be made finite to all orders in perturbation theory, based on the principle of reduction of couplings. The latter consists in searching for renormalization group invariant relations among parameters of a renormalizable theory holding to all orders in perturbation theory. FUTs have proven very successful so far. In particular, they predicted the top quark mass one and half years before its experimental discovery, while around five years before the Higgs boson discovery a particular FUT was predicting the light Higgs boson in the mass range  $\sim 121 - 126$  GeV, in striking agreement with the discovery at LHC. Here we review the basic properties of the supersymmetric theories and in particular finite theories resulting from the application of the method of reduction of couplings in their dimensionless and dimensionful sectors. Then we analyse the phenomenologically favoured FUT, based on SU(5). This particular FUT leads to a finiteness constrained version of the MSSM, which naturally predicts a relatively heavy spectrum with coloured supersymmetric particles above 2.7 TeV, consistent with the non-observation of those particles at the LHC. The electroweak supersymmetric spectrum starts below 1 TeV and large parts of the allowed spectrum of the lighter might be accessible at CLIC. The FCC-hh will be able to fully test the predicted spectrum.

IFT-UAM/CSIC-18-013

---

\*email: Sven.Heinemeyer@cern.ch

†email: myriam@fisica.unam.mx

‡email: patellis@central.ntua.gr

§email: ntrac@central.ntua.gr

¶email: George.Zoupanos@cern.ch



# $X(5568)$ as a $B\bar{K}$ molecule in the Bethe-Salpeter equation approach in the heavy quark limit

Zhen-Yang Wang <sup>\*</sup>, Jing-Juan Qi <sup>†</sup>, and Xin-Heng Guo <sup>‡</sup>

*College of Nuclear Science and Technology, Beijing Normal University, Beijing 100875, China*

Chao Wang <sup>§</sup>

*Center for Ecological and Environmental Sciences,*

*Key Laboratory for Space Bioscience & Biotechnology,*

*Northwestern Polytechnical University, Xi'an 710072, China*

(Dated: February 14, 2018)

## Abstract

In the heavy quark limit, we study the  $X(5568)$  state as a  $B\bar{K}$  molecule in the Bethe-Salpeter equation approach. With the kernel containing one-particle-exchange diagrams, we solve the Bethe-Salpeter equation numerically in the covariant instantaneous approximation and find that the  $X(5568)$  can exist as a  $B\bar{K}$  molecular state with quantum numbers  $I(J^P) = 1(0^+)$ . In this picture we calculate the strong decay width of  $X(5568) \rightarrow B_s^0 \pi^+$  and find it to be in the range 19.83 - 22.45 MeV, which is consistent with the experimental data from the D0 Collaboration.

PACS numbers: 11.10.St, 12.39.Hg, 12.39.Fe, 13.75.Lb

---

<sup>\*</sup> e-mail: wangz-y@mail.bnu.edu.cn

<sup>†</sup> e-mail: qijj@mail.bnu.edu.cn

<sup>‡</sup> Corresponding author, e-mail: xhguo@bnu.edu.cn

<sup>§</sup> Corresponding author, e-mail: chaowang@nwpu.edu.cn

# The minimal type-I seesaw model with maximally-restricted texture zeros

D. M. Barreiros,<sup>1</sup> R. G. Felipe,<sup>1,2</sup> and F. R. Joaquim<sup>1</sup>

<sup>1</sup>*Departamento de Física and CFTP, Instituto Superior Técnico, Universidade de Lisboa, Lisboa, Portugal*

<sup>2</sup>*Instituto Superior de Engenharia de Lisboa, Rua Conselheiro Emídio Navarro, 1959-007 Lisboa, Portugal*

In the context of Standard Model (SM) extensions, the seesaw mechanism provides the most natural explanation for the smallness of neutrino masses. In this work we consider the most economical type-I seesaw realization in which two right-handed neutrinos are added to the SM field content. For the sake of predictability, we impose the maximum number of texture zeros in the lepton Yukawa and mass matrices. All possible patterns are analyzed in the light of the most recent neutrino oscillation data, and predictions for leptonic CP violation are presented. We conclude that, in the charged-lepton mass basis, eight different texture combinations are compatible with neutrino data at  $1\sigma$ , all of them for an inverted-hierarchical neutrino mass spectrum. Four of these cases predict a CP-violating Dirac phase close to  $3\pi/2$ , which is around the current best-fit value from global analysis of neutrino oscillation data. If one further reduces the number of free parameters by considering three equal elements in the Dirac neutrino Yukawa coupling matrix, several texture combinations are still compatible with data but only at  $3\sigma$ . For all viable textures, the baryon asymmetry of the Universe is computed in the context of thermal leptogenesis, assuming (mildly) hierarchical heavy Majorana neutrino masses  $M_{1,2}$ . It is shown that the flavored regime is ruled out, while the unflavored one requires  $M_1 \sim 10^{14}$  GeV.

## I. INTRODUCTION

The discovery of neutrino oscillations provided a solid evidence for physics beyond the Standard Model (SM), by confirming the existence of neutrino masses and mixing. From the theory viewpoint, the most straightforward and elegant way of accounting for them consists of adding right-handed (RH) neutrinos to the SM field content. If heavy enough, these states can mediate neutrino masses at the classical level through the well-known seesaw mechanism [1]. Besides supplying an explanation for small neutrino masses, the addition of RH neutrinos to the SM allows for the leptogenesis mechanism [2] to work through the out-of-equilibrium decays of the heavy neutrinos in the early Universe (for reviews see e.g. [3–6]). This offers an answer for another SM puzzle: the baryon asymmetry of the Universe (BAU).

Although, in principle, the number of RH neutrinos is arbitrary, at least two are necessary to explain the present neutrino oscillation data, namely, three nonzero neutrino mixing angles and two mass-squared differences. Interestingly, at least two RH neutrinos are also required for leptogenesis to be realized. Therefore, the two RH neutrino seesaw model (2RHNSM) is not only a minimal model for neutrino masses, but also for the generation of the BAU in the context of leptogenesis. Still, even in this scenario, the number of parameters describing the neutrino Lagrangian at high energies is larger than the number of low-energy observables currently (or potentially) measured by experiments. One way of increasing predictability is to consider texture zeros in the lepton Yukawa and mass matrices, which can be motivated, for instance, by imposing U(1) Abelian flavor symmetries [7, 8]. In general, texture zeros imply predictions not only for low-energy neutrino parameters but also for the BAU, since leptogenesis is sensitive to the couplings which control neutrino masses and mixing. Therefore, a

complete study of all possible texture zeros in the light of most recent neutrino data is welcome. In particular, since neutrino experiments are starting to deliver some information regarding leptonic CP violation [9], predictions for low-energy CP phases are of utmost importance. At the same time, a connection with leptogenesis can also be established in this framework [9, 10]. These questions have already been partially covered in the literature. For instance, the compatibility of texture-zero hypothesis in the 2RHNSM with neutrino data has been studied in Refs. [11–15] and, in the context of leptogenesis, in Refs. [16–23].

In this work, we revisit the 2RHNSM in maximally restricted texture-zero scenarios, i.e. when the maximum number of texture zeros is imposed in the lepton Yukawa and mass matrices. Moreover, we consider cases in which equality relations among the Dirac neutrino Yukawa couplings exist. For textures that reproduce the observed neutrino mass and mixing patterns, we present the predictions for low-energy CP violation, neutrinoless double beta decay and the BAU. Special attention will be paid to the treatment of leptogenesis in the 2RHNSM. Contrary to what is usually done in the literature, where only the decay of the lightest heavy neutrino is considered, we include decays of both heavy neutrinos in our analysis. Moreover, flavor effects which arise from the fact that lepton interactions become out of equilibrium at different temperatures are taken into account.

This paper is organized as follows. In Section II we set the basics of the 2RHNSM, by describing the model and identifying the number of parameters at high and low energies. Afterwards, in Section III, the maximally-restricted texture zero matrices are identified, and their compatibility with neutrino data is analyzed. Furthermore, the predictions for Dirac and Majorana CP phases are shown, together with those for the effective neutrino mass parameter relevant for neutrinoless double beta de-

Nisha Dhiman · Harleen Dahiya

# Ratios of vector and pseudoscalar $B$ meson decay constants in the light-cone quark model

Received: date / Accepted: date

**Abstract** We study the decay constants of pseudoscalar and vector  $B$  meson in the framework of light-cone quark model (LCQM). We apply the variational method to the relativistic Hamiltonian with the Gaussian-type trial wave function to obtain the values of  $\beta$  (scale parameter). Then with the help of known values of constituent quark masses, we obtain the numerical results for the decay constants  $f_P$  and  $f_V$ , respectively. We compare our numerical results with the existing experimental data.

**Keywords** Light-cone quark model · Decay constant

## 1 Introduction

The study of the decay constants of heavy mesons is very important, since it provides a direct source of information on the Cabibbo-Kobayashi-Maskawa (CKM) matrix elements which describe the couplings of the third generation of quarks to the lighter quarks. These matrix elements are the fundamental parameters of the Standard Model (SM) and their precise measurement will allow us to test the unitarity of the quark mixing matrix and  $CP$  violation in the SM [1]. However, the uncertainty in the knowledge of the decay constant make it difficult to extract precisely the CKM matrix elements from the experimental data. For example, in the lowest order approximation, the decay widths of the pseudoscalar and vector mesons can be written as [2]

$$\begin{aligned}\Gamma(P \rightarrow \ell\nu) &= \frac{G_F^2}{8\pi} f_P^2 m_\ell^2 m_P \left(1 - \frac{m_\ell^2}{m_P^2}\right)^2 |V_{qQ}|^2, \quad \text{and} \\ \Gamma(V \rightarrow \ell\nu) &= \frac{G_F^2}{12\pi} f_V^2 m_V^3 \left(1 - \frac{m_\ell^2}{m_V^2}\right)^2 \left(1 + \frac{m_\ell^2}{2m_V^2}\right) |V_{qQ}|^2.\end{aligned}\tag{1}$$

The experimental measurements of purely leptonic decay branching fractions and their lifetimes allow us to determine the product  $f_P|V_{qQ}|$  ( $f_V|V_{qQ}|$ ). Thus, a precise theoretical input on  $f_{P(V)}$  can allow a determination of the CKM matrix element. The theoretical calculations of the decay constants of  $B$  mesons require non-perturbative treatment since at short distances, the interactions are dominated by strong force. There have been many theoretical groups that are working on the calculation of the decay constants in the realm of non-perturbative QCD using different models. Here we focus on one such method that is useful for solving non-perturbative problems of hadron physics: the light-cone quark

---

Authors would like to thank the Department of Science and Technology (Ref No. SB/S2/HEP-004/2013) Government of India for financial support.

---

N. Dhiman · H. Dahiya  
 Dr. B. R. Ambedkar National Institute of Technology, Jalandhar, India  
 E-mail: nishdhiman1292@gmail.com

# Polarization observables and T-noninvariance in the weak charged current induced electron proton scattering

A. Fatima,<sup>1</sup> M. Sajjad Athar,<sup>1,\*</sup> and S. K. Singh<sup>1</sup>

<sup>1</sup>*Department of Physics, Aligarh Muslim University, Aligarh-202002, India*

In this work, we have studied the total scattering cross section ( $\sigma$ ), differential scattering cross section ( $d\sigma/dQ^2$ ) as well as the longitudinal ( $P_L(E_e, Q^2)$ ), perpendicular ( $P_P(E_e, Q^2)$ ), and transverse ( $P_T(E_e, Q^2)$ ) components of the polarization of the final hadron ( $n$ ,  $\Lambda$  and  $\Sigma^0$ ) produced in the electron proton scattering induced by the weak charged current. We have not assumed T-invariance which allows the transverse component of the hadron polarization perpendicular to the production plane to be non-zero. The numerical results are presented for all the above observables and their dependence on the axial vector form factor and the weak electric form factor are discussed. The present study enables the determination of the axial vector nucleon-hyperon transition form factors at high  $Q^2$  in the strangeness sector which can provide test of the symmetries of the weak hadronic currents like T-invariance and SU(3) symmetry while assuming the hypothesis of conserved vector current and partial conservation of axial vector current.

PACS numbers: 12.15.Ji, 13.88.+e, 14.20.Jn, 14.60.Cd

## I. INTRODUCTION

The study of the nucleon polarizations in the elastic scattering of electron from the (un)polarized proton targets has made important contributions to our present understanding of the electromagnetic form factors of the nucleons in the region of high  $Q^2$  [1, 2]. In the case of the neutrino-nucleon scattering processes induced by the weak charged currents, various suggestions have been made in the past by many authors that the polarization measurements of the leptons and hadrons produced in the final state along with the measurements of the differential cross sections can provide a determination of all the weak nucleon form factors [3–20]. A precise determination of these form factors in the (anti)neutrino-nucleon scattering would facilitate the study of various symmetry properties and conservation laws associated with the weak hadronic currents in the  $\Delta S = 0$  and  $\Delta S = 1$  sectors.

While discussing the importance of the polarization measurements in the (anti)neutrino-nucleon scattering in the development of the weak interaction theory, some of the earlier works [4, 5, 15–18] have emphasized the technical challenges and difficulties involved in making such polarization measurements of the final nucleon in reactions like  $\bar{\nu}_\mu + p \rightarrow \mu^+ + n$  and  $\nu_\mu + n \rightarrow \mu^- + p$  with the experimental facilities then available at the CERN and other laboratories involved in doing (anti)neutrino scattering experiments. In this context, it was suggested that the observation of the final hadron polarizations may be feasible if a hyperon ( $\Lambda$  or  $\Sigma^0$ ) is produced in the quasielastic antineutrino-nucleon reactions like  $\bar{\nu}_\mu + p \rightarrow \mu^+ + \Lambda(\Sigma^0)$  [6, 14, 16–18, 21]. This is because the  $\Lambda$  or  $\Sigma^0$  produced in these reactions decay into pions and the asymmetry in the angular distribution of the pions with respect to a given direction depends upon the polarization of  $\Lambda$  or  $\Sigma^0$  in that direction. Therefore, an observation of the asymmetry in the angular distribution of the pions determines directly the polarization of  $\Lambda(\Sigma^0)$ . Indeed, an experiment to study the quasielastic hyperon production performed at CERN with the SPS antineutrino beam has reported the results on the longitudinal, perpendicular and transverse polarizations of  $\Lambda$  [22] along with the cross section measurements while the other experiments performed at CERN, BNL, FNAL and SKAT have published their results only on the cross section measurements [23–28]. However, the experimental uncertainties quoted in the values of the form factors determined in the axial vector sector were quite large due to the poor statistics of the observed  $\Lambda$  events.

In recent years, there has been considerable development in the field of experimental neutrino physics with the availability of high intensity neutrino beams and technical advances in designing the large volume detectors to study the physics of neutrino oscillations. The specific experimental programs dedicated to make such studies also plan to perform (anti)neutrino-nucleon cross section measurements in the near detector for various reaction channels in the scattering of (anti)neutrinos from the nuclear targets [29–32]. These experiments may also be able to study the hyperon production with better statistics and perform the polarization measurements for the final leptons and hadrons. In this context, there have been many theoretical calculations of the polarization observables of the final leptons and hadrons in the (anti)neutrino-nucleon scattering processes [33–42].

---

\*Electronic address: [sajathar@gmail.com](mailto:sajathar@gmail.com)

# On the light massive flavor dependence of the top quark mass

**André H. Hoang**  
University of Vienna, Vienna, AUSTRIA  
E-mail: andre.hoang@univie.ac.at

**Christopher Lepenik\***  
University of Vienna, Vienna, AUSTRIA  
E-mail: christopher.lepenik@univie.ac.at

**Moritz Preisser**  
University of Vienna, Vienna, AUSTRIA  
E-mail: moritz.preisser@univie.ac.at

We provide a systematic renormalization group formalism to study the mass effects in the relation of the pole mass and short-distance masses such as the  $\overline{\text{MS}}$  mass of a heavy quark  $Q$ , coming from virtual loop insertions of massive quarks lighter than  $Q$  with the main focus on the top quark. The formalism reflects the constraints from heavy quark symmetry and entails a combined matching and evolution procedure that allows to disentangle and successively integrate out the corrections coming from the lighter massive quarks and the momentum regions between them and also to precisely control the large order asymptotic behavior. The formalism is used to study the asymptotic behavior of light massive flavor contributions and is applied to predict the  $\mathcal{O}(\alpha_s^4)$  virtual quark mass corrections, calculate the pole mass differences for massive quark flavors with a precision of around 20 MeV, and determine the pole mass ambiguity which amounts to 250 MeV in the physical case of three massless quark flavors.

13th International Symposium on Radiative Corrections (Applications of Quantum Field Theory to Phenomenology)  
25-29 September, 2017  
St. Gilgen, Austria

\*Speaker.

© Copyright owned by the author(s) under the terms of the Creative Commons Attribution-NonCommercial-NoDerivatives 4.0 International License (CC BY-NC-ND 4.0).

<https://pos.sissa.it/>

On the light massive flavor dependence of the top quark mass

Christopher Lepenik

## 1. Introduction

The masses of the heavy quarks, especially of the top, are among the most important parameters in the standard model, having strong impact on e.g. precise consistency tests of the standard model and the estimation of the electroweak vacuum stability. However, it must be kept in mind that the mass of a heavy quark  $Q$ , due to confinement, is not a physical observable but should be viewed as a formal theory parameter which depends on the renormalization scheme. Depending on the observable and energy scale of interest different renormalization schemes are used in calculations to minimize theoretical uncertainties. Therefore it is necessary to determine precise relations between the several mass renormalization schemes such that accurate comparisons can be made between them.

Considering the pole mass scheme, it is well known that the resulting mass parameter  $m_Q^{\text{pole}}$  is linearly sensitive to small momenta and hence sensitive to the non-perturbative regime of QCD. This low momentum sensitivity even grows rapidly with loop order and leads to the so-called  $\mathcal{O}(\Lambda_{\text{QCD}})$  renormalon [1–3]. On the other hand there are “short-distance masses” like the  $\overline{\text{MS}}$ , kinetic [4], PS [5], 1S [6–8], RS [9], and MSR [10, 11] masses which have no linear low momentum sensitivity and consequently do not have such a renormalon. The  $\overline{\text{MS}}$  mass  $\overline{m}_Q(\mu)$  is defined analogous to the  $\overline{\text{MS}}$ -renormalized strong coupling constant  $\alpha_s(\mu)$ . Like the strong coupling, the  $\overline{\text{MS}}$  mass  $\overline{m}_Q(\mu)$  depends on a renormalization scale  $\mu$  which should be parametrically of the order or higher than the mass scale itself. In the case of the  $\overline{\text{MS}}$  mass this scale can be interpreted as the scale above which short-distance information from on-shell self-energy diagrams is contained in the mass. So the difference between  $\overline{\text{MS}}$  and pole mass,  $m^{\text{pole}} - \overline{m}_Q(\mu)$ , contains these self-energy contributions between momentum zero and the scale  $\mu$ .

In the approximation that all flavors lighter than the heavy quark  $Q$  are massless the relation between the pole and  $\overline{\text{MS}}$  mass can be written in the form

$$m_Q^{\text{pole}} - \overline{m}_Q = \overline{m}_Q \sum_{n=1}^{\infty} a_n(n_Q, n_h) \left( \frac{\alpha_s^{(n_Q+n_h)}(\overline{m}_Q)}{4\pi} \right)^n, \quad (1.1)$$

where  $\overline{m}_Q \equiv \overline{m}_Q(\overline{m}_Q)$ ,  $n_Q$  is the number of quark flavors lighter than  $\overline{m}_Q$  (which are taken massless at this point),  $n_h$  is the number of quark flavors with mass  $\overline{m}_Q$ , and  $\alpha_s^{(n_Q+n_h)}$  is the strong coupling constant that evolves with  $n_Q + n_h$  active dynamical flavors according to the evolution equation

$$\frac{d\alpha_s^{(n_Q)}(\mu)}{d\log\mu} = \beta^{(n_Q)}(\alpha_s(\mu)) = -2\alpha_s^{(n_Q)}(\mu) \sum_{n=0}^{\infty} \beta_n^{(n_Q)} \left( \frac{\alpha_s^{(n_Q)}(\mu)}{4\pi} \right)^{n+1}. \quad (1.2)$$

The perturbative coefficients  $a_n(n_Q, n_h)$  are known up to  $\mathcal{O}(\alpha_s^4)$  from explicit loop calculations [12–19]. Owing to their renormalon behavior, they are known asymptotically to all orders through formulas like [3, 11]

$$a_n^{\text{asy}}(n_Q, n_h) = a_n^{\text{asy}}(n_Q, 0) = 4\pi N_{1/2}^{(n_Q)} (2\beta_0^{(n_Q)})^{n-1} \sum_{k=0}^{\infty} \frac{g_k^{(n_Q)} \Gamma(n + \hat{b}_1^{(n_Q)} - k)}{\Gamma(1 + \hat{b}_1^{(n_Q)})}, \quad (1.3)$$

where  $g_k$  and  $\hat{b}_1$  are polynomials of the QCD  $\beta$ -function coefficients  $\beta_n$  (see Eq. (1.2)) and the anomalous dimension of the  $\overline{\text{MS}}$  mass [11], and  $N_{1/2}^{(n_Q)}$  is a normalization [11, 20, 21]. Numerically,

# $\eta$ and $\omega$ mesons as new degrees of freedom in the intranuclear cascade model INCL

J.-C. David<sup>1</sup>, A. Boudard<sup>1</sup>, J. Cugnon<sup>2</sup>, J. Hirtz<sup>1,3</sup>, S. Leray<sup>1</sup>, D. Mancusi<sup>4</sup>, and J. L. Rodriguez-Sanchez<sup>1</sup>

<sup>1</sup> Irfu, CEA, Université Paris-Saclay, 91191 Gif-sur-Yvette, France

<sup>2</sup> University of Liège, AGO Department, allée du 6 août 17, Bât. B5, B-4000 Liège 1, Belgium

<sup>3</sup> Center for Space and Habitability, Universität Bern, CH-30 12 Bern, Switzerland

<sup>4</sup> Den-Servise d'étude des réacteurs et de mathématiques appliquées (SERMA), CEA, Université Paris-Saclay, 91191 Gif-sur-Yvette, France

the date of receipt and acceptance should be inserted later

**Abstract.** The intranuclear cascade model INCL (Liège Intranuclear Cascade) is now able to simulate spallation reactions induced by projectiles with energies up to roughly 15 GeV. This was made possible thanks to the implementation of multipion emission in the NN,  $\Delta$ N and  $\pi$ N interactions. The results obtained with reactions on nuclei induced by nucleons or pions gave confidence in the model. A next step will be the addition of the strange particles,  $\Lambda$ ,  $\Sigma$  and Kaons, in order to not only refine the high-energy modeling, but also to extend the capabilities of INCL, as studying hypernucleus physics. Between those two versions of the code, the possibility to treat the  $\eta$  and  $\omega$  mesons in INCL has been performed and this is the topic of this paper. Production yields of these mesons increase with energy and it is interesting to test their roles at higher energies. More specifically, studies of  $\eta$  rare decays benefit from accurate simulations of its production. These are the two reasons for their implementation. Ingredients of the model, like elementary reaction cross sections, are discussed and comparisons with experimental data are carried out to test the reliability of those particle productions.

**PACS.** XX.XX.XX No PACS code given

## 1 Introduction

Nuclear reactions between a light particle (*e.g.* hadron) and a nucleus have been extensively studied. In the last twenty years, for incident energies from  $\sim 100$  MeV up to a few GeV, great improvements were obtained, as shown by the two international benchmarks carried out in mid-nineties [1,2] and 2010 [3]. The studies of those reactions, which take place in space due to the cosmic rays as well as in accelerators, has been triggered mostly by transmutation of nuclear wastes. This explains the energy domain and the focus on residual nucleus and neutron production, even if light charged particles (proton, deuteron, ..., and also pion) were also studied. Some codes can already simulate those types of reactions for higher incident energies, taking into account other particles than nucleons and pions, since new particles appear when energy increases. Around say 10 GeV two groups of models can be used to reproduce these reactions. A first group includes the high energy models, often based on a String model (*e.g.* [4,5], from the TeV (or higher) down to a few GeV, and a second group with the BUU (*e.g.* [6,7,8]), QMD (*e.g.* [9,10,11,12]) and intranuclear cascade (INC) (*e.g.* see Table 1 in [13]) models where the extension to higher energies needs new ingredients.

This article is about the extension of the intranuclear cascade model INCL toward the high energies (10-15 GeV). In 2011 S. Pedoux and J. Cugnon [14] did the main part of the work by implementing the multiple pion production processes in the elementary interactions (NN,  $\Delta$ N and  $\pi$ N). The idea rested on the two facts that i) when the energy goes up new particles are produced, *i.e.* especially new resonances, which will decay mainly in pions and nucleon in a time much shorter than the duration of the cascade, and ii) information on those resonances (masses, widths, related cross sections) are not always well known and moreover overlaps exist between resonances making the choice awkward. This multipion production model in INCL [15,16] leads to good results regarding pion production [17] compared to experimental data and to other models.

Nevertheless, even though pions are the main particles produced, some others like  $\eta$  and  $\omega$  mesons and the strange particles (kaons and hyperons) can appear as well. Implementation of these particles should not significantly change the global features of the reactions (residual nucleus, neutron and light charged particle production), but first this has to be confirmed, and second those particles can be new fields of study. Considering strange particles, hypernuclei can

# Benchmark of the GEF model for fission-fragment yields over an enlarged range

C. Schmitt,<sup>1,\*</sup> K.-H. Schmidt,<sup>2</sup> and B. Jurado<sup>2</sup>

<sup>1</sup>*IPHC CNRS/IN2P3, 23 rue du Loess, B.P. 28, F-67037 Strasbourg, France*

<sup>2</sup>*CENBG CNRS/IN2P3, Chemin du Solarium, B.P. 120, F-33175 Gradignan, France*

(Dated: February 14, 2018)

The GEneral description of Fission observables (GEF) model was developed to produce fission-related nuclear data which are of crucial importance for basic and applied nuclear physics. The investigation of the performance of the GEF code is here extended to a region in fissioning-system mass, charge, excitation energy and angular momentum, as well as to new observables, that could not be benchmarked in detail so far. The work focuses on fragment mass and isotopic distributions, benefiting from recent innovative measurements. The approach reveals a high degree of consistency and provides a very reasonable description of the new data. The physics behind specific discrepancies is discussed, and hints to improve on are given. Comparison of the calculation with experiment permits to highlight the influence of the system intrinsic properties, their interplay, and the importance of experimental aspects, namely instrumental resolution. All together points to the necessity of as selective and accurate as possible experimental data, for proper unfolding of the different influences and robust interpretation of the measurement. The GEF code has become a widely used tool for this purpose.

PACS numbers: 24.10.-i, 25.85.-w, 25.85.Ec, 25.85.Ge

## I. INTRODUCTION

The evolution of a nucleus from a compact configuration into two separated fragments is an intricate puzzle, and it remains a challenge to unambiguously unfold the influence of the various aspects which enter in play. At the same time, the fission process constitutes a rich laboratory for investigating fundamental nuclear properties [1], and it is of key importance in applied science, including safeguards, accelerator technology, homeland security, medicine, energy production and waste transmutation at nuclear reactors [2]. Fission is also an important process in astrophysical context [3]. Modeling fission, in general, implies (i) the definition of the initial conditions as determined by the entrance-channel reaction, (ii) the decay of the fissioning nucleus and its re-arrangement in specific configurations of fragment pairs with corresponding probabilities, (iii) the (prompt) de-excitation of the excited fragments, and (iv) the (slow) decay of the radioactive species towards stability. Models dedicated to fundamental purposes restrict to the first three items, while codes for applications and astrophysics need to cover all aspects. In addition, they need to be computationally fast and flexible, for efficient implementation in general-purpose transport codes modeling the interaction of radiation with nearly everything (see Refs. [4, 5]). Models oriented in the direction of describing the process starting from fundamental principles and quantum mechanics (see Refs. [7–10]) tremendously developed during the last years. Unfortunately, they cannot afford yet the predictive-power specifications for applied science,

and computing time is still prohibitive for large-scale calculations. In parallel, intense work was invested in the development of models and codes suited for use in *e.g.* experimental data analysis, data evaluation, applications and astrophysics. They are of various types, going from parameterized systematics [12] to more or less phenomenological or (semi-)empirical models, see Refs. [11, 13–18] and therein. The present work investigates the performance of one of these models, the GEneral description of Fission observables (GEF) model [17], over an extended range of fissioning systems.

The GEF code is a semi-empirical model for the description of a (nearly exhaustive) list of fission observables. It combines a set of equations exploiting ideas of quantum mechanics, nuclear dynamics, and statistical mechanics, with a unique set of parameters which were adjusted once to a comprehensive set of experimental data. A particularly rich variety of experimental observations enters the adjustment procedure, including fission excitation functions, fragment properties in mass  $A$ , charge  $Z$ , kinetic energy  $E_{kin}$ , emitted-neutron  $\nu$  and  $\gamma$ -ray multiplicity distributions and energy spectra. This variety is a key point for reaching a consistent description, due to the (sometimes far-reaching) correlations that exist between fission observables. To illustrate the impact of this inter-dependence, we quote an example: The amount and energy of the (prompt and delayed) neutrons are straightforwardly related to the final fragment residues. The latter depend on the so-called pre-neutron fragment ( $A$ ,  $Z$ ) population right after scission, and their excitation energy. The pre-neutron products are determined by, among others, the fragment binding energies, and the generation and sharing of excitation energy at scission. Hence, information about neutron multiplicities and energies can impact the modeling of

---

\*Electronic address: christelle.schmitt@iphc.cnrs.fr